Med Chem Res (2012) 21:1451–1470
DOI 10.1007/s00044-011-9662-9

MEDICINAL CHEMISTRY RESEARCH

ORIGINAL RESEARCH

# Isonicotinic acid hydrazide derivatives: synthesis, antimicrobial activity, and QSAR studies

**Vikramjeet Judge · Balasubramanian Narasimhan · Munish Ahuja · Dharmarajan Sriram · Perumal Yogeeswari · Erik De Clercq · Christophe Pannecouque · Jan Balzarini**

Received: 10 March 2011 / Accepted: 5 May 2011 / Published online: 21 May 2011


**Abstract** A series of isonicotinic acid hydrazide derivatives (**1**–**19**) was synthesized and tested in vitro for antimycobacterial activity against *Mycobacterium tuberculosis* and antimicrobial activity against *Staphylococcus aureus, Bacillus subtilis, Escherichia coli, Candida albicans, and Aspergillus niger* and the results indicated that the compounds with OH, $SCH_3$, and $OCH_3$ groups were found to be active against the tested strains. None of the test compounds were active against a broad variety of RNA and DNA viruses at subtoxic concentrations, except **8**, that showed some selective anti-reovirus-1 activity. The multi-target QSAR models were found to be effective in predicting the antimicrobial activity of the isoniazid derivatives and indicated the importance of nuclear repulsion energy (Nu.E) in explaining the antimicrobial activity of isoniazid derivatives. The developed QSAR models were validated using the external test set of synthesized derivatives.

V. Judge · M. Ahuja
Department of Pharmaceutical Sciences, Guru Jambheswar University of Science and Technology, Hisar 125001, India

B. Narasimhan (✉)
Faculty of Pharmaceutical Sciences, Maharshi Dayanand University, Rohtak 124001, India
e-mail: naru2000us@yahoo.com

D. Sriram · P. Yogeeswari
Medicinal Chemistry Research Laboratory, Pharmacy Group, Birla Institute of Technology and Science, Hyderabad 500078, India

E. De Clercq · C. Pannecouque · J. Balzarini
Laboratory of Virology & Chemotherapy, Rega Institute for Medical Research, Minderbroedersstraat 10, 3000 Leuven, Belgium

**Keywords** Isoniazid derivatives · Antimycobacterial · Antiviral · Antimicrobial · QSAR

## Introduction

Tuberculosis (TB), caused by the infectious agent *Mycobacterium tuberculosis*, is one of the most important killing infectious diseases. According to alarming data from the World Health Organization (WHO), TB has spread to every corner of the globe. As much as one third of the world's population is currently infected, and more than 5,000 people die from TB everyday (Sriram *et al.*, 2009). The factors responsible for this are: (i) patient non-compliance to existing drug regimens which has resulted in the emergence of single drug-resistant strains to all major anti-TB drugs; (ii) emergence of multidrug-resistant TB (MDR-TB), which is defined as the disease caused by the strains of *M. tuberculosis* resistant to two mainstay first-line anti-TB drugs, isoniazid and rifampicin; and (iii) association of human immunodeficiency virus (HIV) with TB, in which TB is the leading cause of death among patients who are HIV-positive. Consequently, new drugs with divergent and unique structure and with a mechanism of action possibly different from that of existing drugs are urgently required (Nayyar *et al.*, 2007).

AIDS is caused by a retrovirus, the human immunodeficiency virus (HIV). Two genetically distinct subtypes (HIV-1 and HIV-2) have been characterized, but it is known that the prime etiological agent of AIDS is HIV-1 (Canoa *et al.*, 2006). Combination therapy or highly active antiretroviral therapy (HAART) with two or more reverse transcriptase inhibitors and protease inhibitors (PIs) has dramatically improved the quality of life and survival of patients infected with human immunodeficiency virus

(HIV) type 1 (HIV-1). However, the ability to provide effective long-term antiretroviral therapy for HIV-1 infection has become a complex issue, since 40–50% of those who initially achieved favorable viral suppression to undetectable levels have experienced treatment failure (Koh *et al.*, 2003).

In the past 25 years, the incidence of microbial infections has increased an alarming level over the world as result of antimicrobial resistance. A growing number of immuno-compromised patients are as a result of cancer chemotherapy, organ transplantation, and HIV infection which are the major factors contributing to this increase. The health problems demand to search and synthesize a new class of antimicrobial compounds effective against pathogenic microorganisms that developed resistance to the antibiotics used in the current regimen (Bayrak *et al.*, 2009a).

Quantitative structure–activity relationship (QSAR) research has been considered a major tool in drug discovery to explore the ligand receptor/enzyme interactions, especially when the structural details of the target are not known. QSAR is an effective way for optimizing or correlating the biological activity within a congeneric series with certain structural features or with functional determinants, such as lipophilicity, polarizability, or electronic and steric properties (Sivaprakasam *et al.*, 2006). QSAR models are mathematical equations which construct a relationship between chemical structures and their biological activities as a linear regression model of the form $y = Xb + e$. This equation may be used to describe a set of predictor variables ($X$) with a predicted variable ($y$) by means of a regression vector ($b$). In a typical QSAR study one needs to find a set of molecular descriptors representing the higher impact on the biological activity of interest (Sabet *et al.*, 2010).

Isonicotinic acid hydrazide (Isoniazid; INH) and pyrazinamide (PZA) are widely applied as a first line drugs for the treatment of tuberculosis, usually in combination with other drugs. Modifying either of these molecules has been a challenge taken up by several research groups (Imramovsky *et al.*, 2007). Furthermore, the pharmacokinetic properties and cellular permeability of a drug can be modulated by derivatization to bioreversible forms of this drug, namely hydrazones (Sriram *et al.*, 2006). Isoniazid derivatives have been reviewed by Scior and Garces-Eisele (2006) and antitubercular evaluation of novel series of 3-benzofuran-5-aryl-1-pyrazolyl-pyridylmethanone analogs derived from isoniazid have been reported (Manna and Agrawal, 2010). Recently, antimicrobial properties of isoniazid have also been studied (Bayrak *et al.*, 2009a, b; Rodriguez-Arguelles *et al.*, 2007). In light of above facts and in continuation of our research endowed toward the synthesis, antimicrobial, antimycobacterial, antiviral, and QSAR studies (Judge *et al.*, in press; Kumar *et al.*, 2010a, b), we hereby report the synthesis, antitubercular, anti-HIV, antimicrobial, and QSAR studies of isoniazid derivatives.

## Experimental

Melting points were determined in open capillary tubes on a Sonar melting point apparatus and are uncorrected. Reaction progress was monitored by thin layer chromatography on silica gel sheets (Merck silica gel-G) and the purity of the compounds was ascertained by single spot on TLC sheet. $^1$H nuclear magnetic resonance ($^1$H NMR) spectra were recorded in Bruker Avance II 400 NMR spectrometer using appropriate deuterated solvents and are expressed in parts per million ($\delta$, ppm) downfield from tetramethylsilane (internal standard). Infrared (IR) spectra were recorded on a Shimadzu FTIR spectrometer.

### General procedure for synthesis of ester of isonicotinic acid

The mixture of isonicotinic acid (0.1 mol) and ethanol (in excess) was refluxed with sulfuric acid (1–2 ml) till the completion of reaction monitored by TLC on silica gel G plates. Then the reaction mixture was added to 200 ml ice cold water and excess of acid was neutralized by a solution of sodium bicarbonate. The crude ester was extracted with ether. The ether layer was separated and ester was obtained on evaporation of ether layer.

### General procedure for the synthesis of isonicotinic acid hydrazide

The ethanolic solution of ester (0.01 mol) and hydrazine-hydrate (0.015 mol) was refluxed for appropriate time. The reaction mixture was then cooled and the precipitated solid was washed with water, dried, and recrystallized from ethanol.

### General procedure for the synthesis of schiff bases of isoniazid

The solution of isonicotinic acid hydrazide (0.01 mol) and appropriate substituted aldehyde (0.01 mol) in ethanol was refluxed for 4–5 h. The precipitates obtained were filtered off, washed, and recrystallized from ethanol.

#### *Isonicotinic acid -3-ethoxy-4-hydroxybenzylidene hydrazide (**1**)*

Mp (°C) above 242; Yield—65.3%; $^1$H NMR (400 MHz, $CDCl_3$) $\delta$ ppm: 3.87 (t, 3H, $CH_3$), 4.17–4.20 (q, 2H, $CH_2$),

6.89–6.91 (s, 1H, OH), 7.06–7.08 (s, 1H, CH of $C_2$ of phenyl ring), 7.97 (d, 2H, CH of $C_5$ and $C_6$ of phenyl ring), 8.37 (d, 2H, CH of $C_2$ and $C_6$ of pyridine ring), 8.79 (d, 2H, CH of $C_3$ and $C_5$ of pyridine ring), 11.71 (s, 1H, NH). IR (KBr pellets) $\nu$ $cm^{-1}$: 3254.34 (NH str., amide), 3093.31 (CH str., aromatic), 2973.58 (CH str., aliphatic), 1644.86 (C=O str., amide), 1593.74 (C=C str., skeletal phenyl nucleus), 1276.12 (C–O–C str., aralkyl ether), 1255.95 (OH bending), 845.53 (CH out of plane bending, 4-substituted pyridine).

*Isonicotinic acid-3,4,5-trimethoxybenzylidene hydrazide (**4**)*

Mp (°C) 205–208; Yield—80.7%; $^1$H NMR (400 MHz, DMSO) $\delta$ ppm: 3.36 (s, 9H, $OCH_3$), 7.21–7.23 (s, 2H, CH of $C_2$ and $C_6$ of trimethoxy phenyl ring), 7.83–7.84 (d, 2H, CH of $C_3$ and $C_5$ of pyridine ring), 8.44 (s, 1H, CH of N=CH), 8.73–8.76 (d, 2H, CH of $C_2$ and $C_6$ of pyridine ring), 11.91 (s, 1H, NH). IR (KBr pellets) $\nu$ $cm^{-1}$: 3168.22 (NH str., amide), 2983.04 (CH str., aliphatic), 1682.00 (C=O str., amide), 1583.63 (C=C str., skeletal phenyl nucleus), 1248.96 (C-O-C str., aralkyl ether), 858.36 (CH out of plane bending, 4-substituted pyridine).

*Isonicotinic acid-4-methylbenzylidene hydrazide (**5**)*

Mp (°C) 198–201; Yield—84.6%; $^1$H NMR (400 MHz, DMSO) $\delta$ ppm: 3.28 (s, 3H, $CH_3$), 6.72–6.95 (m, 4H, CH of phenyl ring), 7.76–7.77 (d, 2H, CH of $C_3$ and $C_5$ of pyridine ring), 8.32 (s, 1H, CH of N=CH), 8.68–8.69 (d, 2H, CH of $C_2$ and $C_6$ of pyridine ring), 11.90 (s, 1H, NH). IR (KBr pellets) $\nu$ $cm^{-1}$: 3177.86 (NH str., amide), 2935.78 (CH str., aliphatic), 1682.96 (C=O str., amide), 1583.63 (C=C str., skeletal phenyl nucleus), 1240.0 (C–O–C str., aralkyl ether), 835.21 (CH out of plane bending, 4-substituted pyridine).

*Isonicotinic acid-1-H-indol-3lmethylene hydrazide (**8**)*

Mp (°C) 225–228; Yield—61.9%; $^1$H NMR (400 MHz, DMSO) $\delta$ ppm: 7.07–7.16 (m, 2H, CH of $C_5$ and $C_6$ of indole ring), 7.36–7.38 (m, 2H, CH of $C_4$ and $C_7$ of indole ring), 7.53–7.54 (m, 2H, CH of $C_2$ of indole ring), 7.80–7.81 (d, 2H, CH of $C_3$ and $C_5$ of pyridine ring), 8.60 (s, 1H, CH of N=CH), 8.68–8.71 (d, 2H, CH of $C_2$ and $C_6$ of pyridine ring), 11.24 (s, 1H, NH of indole), 11.57 (s, 1H, NH of hydrazide). IR (KBr pellets) $\nu$ $cm^{-1}$: 3173.04 (NH str., amide), 3052.48 (CH str., aromatic), 2940.61 (CH str., aliphatic), 1634.74 (C=O str., amide), 1428.35 (NH str., indole ring), 739.73 (CH out of plane bending, indole ring), 847.75 (CH out of plane bending, 4-substituted pyridine).

General procedure for the synthesis of $N_1$-benzoylated schiff bases of isoniazid

The Schiff base (0.01 mol) obtained above was dissolved in dichloromethane to which an equimolar amount of benzoyl chloride, obtained by refluxing benzoic acid with thionyl chloride, was added with stirring for 2 h. The crude products were separated out by evaporating dichloromethane and recrystallized from ethanol to yield the pure compounds.

*Benzoic acid N′-(4-hydroxy-3-methoxy-benzylidene)-N-(pyridine-4-carbonyl)-hydrazide (**10**)*

Mp (°C) 230–233; Yield—57.8%; $^1$H NMR (400 MHz, DMSO) $\delta$ ppm: 3.70 (s, 3H, $OCH_3$), 3.84 (s, 3H, OH), 7.28–7.38 (m, 5H, CH of phenyl ring), 7.46–7.50 (m, 3H, CH of benzylidene ring), 7.70 (s, 1H, CH of N=CH), 7.91–7.94 (d, 2H, CH of $C_3$ and $C_5$ of pyridine ring), 8.77 (d, 2H, CH of $C_2$ and $C_6$ of pyridine ring). IR (KBr pellets) $\nu$ $cm^{-1}$: 3414.15 (OH str.), 3036.09 (CH str., aromatic), 2904.92 (CH str., aliphatic), 1680.07 (C=O str., acyl group), 1597.13 (C=O str., amide), 1513.22 (C=C str., skeletal phenyl nucleus), 1285.61 (C–O–C str., aralkyl ether), 814.96 (CH out of plane bending, 4-substituted pyridine).

*Benzoic acid N′-(4-methylsulfanyl-benzylidene)-N-(pyridine-4-carbonyl)-hydrazide (**12**)*

Mp (°C) 226–229; Yield—45.8%; $^1$H NMR (400 MHz, DMSO) $\delta$ ppm: 2.48 (s, 3H, $SCH_3$), 7.11–7.20 (m, 3H, CH of $C_3$, $C_4$ and $C_5$ phenyl ring), 7.34–7.37 (d, 2H, CH of $C_2$, and $C_6$ phenyl ring), 7.62–7.64 (d, 2H, CH of $C_3$ and $C_5$ of benzylidene ring), 7.91–7.93 (d, 2H, CH of $C_2$ and $C_6$ of benzylidene ring), 8.21–8.23 (d, 2H, CH of $C_3$ and $C_5$ of pyridine ring), 8.52 (s, 1H, CH of N=CH), 8.86–8.87 (d, 2H, CH of $C_2$ and $C_6$ of pyridine ring). IR (KBr pellets) $\nu$ $cm^{-1}$: 3014.87 (CH str., aromatic), 1667.53 (C=O str., acyl group), 1596.16 (C=O str., amide), 1497.79 (C=C str., skeletal phenyl nucleus), 609.53 (C–S str.), 732.98 (CH out of plane bending, 4-substituted pyridine).

*Benzoic acid N′-(4-methyl-benzylidene)-N-(pyridine-4-carbonyl)-hydrazide (**14**)*

Mp (°C) 220–223; Yield—62.7%; $^1$H NMR (400 MHz, DMSO) $\delta$ ppm: 2.31 (s, 3H, $CH_3$), 7.07–7.49 (m, 5H, CH of phenyl ring), 7.59–7.61 (d, 2H, CH of $C_3$ and $C_5$ of benzylidene ring), 7.91–7.93 (d, 2H, CH of $C_2$ and $C_6$ of benzylidene ring), 8.56–8.57 (d, 2H, CH of $C_3$ and $C_5$ of pyridine ring), 8.68 (s, 1H, CH of N=CH), 8.93–8.94 (d, 2H, CH of $C_2$ and $C_6$ of pyridine ring). IR (KBr pellets)

$\nu$ $cm^{-1}$: 3004.26 (CH str., aromatic), 1653.07 (C=O str., acyl group), 1593.27 (C=O str., amide), 1486.22 (C=C str., skeletal phenyl nucleus), 841.00 (CH out of plane bending, 4-substituted pyridine).

General procedure for the synthesis of $N_2$-acyl isonicotinic acid hydrazides (**17–19**)

The corresponding carboxylic acids (0.01 mol) were refluxed with thionyl chloride (0.015 mol) for 3 h. After refluxing was complete, the excess thionyl chloride was distilled off to get the acyl chloride. The isonicotinic acid hydrazide (0.01 mol) was suspended in dichloromethane and respective acyl chloride (0.01 mol) was added dropwise to this solution with constant stirring on a magnetic stirrer for 3–4 h. The product obtained after evaporation of dichloromethane was recrystallized from ethanol.

*2-Chloro-5-nitro-benzoic acid N′-(pyridine-4-carbonyl)-hydrazide (**17**)*

Mp (°C) 200–203; Yield—56.30%; $^1$H NMR (400 MHz, DMSO) $\delta$ ppm: 7.79–7.81 (d, 2H, CH of $C_3$ and $C_4$ of phenyl ring), 8.32 (s, 1H, CH of $C_5$ of phenyl ring), 8.51–8.53 (d, 2H, CH of $C_3$ and $C_5$ of pyridine ring), 9.14–9.17 (d, 2H, CH of $C_2$ and $C_6$ of pyridine ring), 10.44 (s, 1H, NH proton of $N_2$), 11.20 (s, 1H, NH proton of $N_1$). IR (KBr pellets) $\nu$ $cm^{-1}$: 3132.53 (NH str., amide), 3083.34 (CH str., aromatic), 1708.04 (C=O str., Nicotinoyl), 1677.18 (C=O str., Acyl), 1528.65 ($NO_2$ asymmetric str., aromatic nitro group), 1339.62 ($NO_2$ symmetric str., aromatic nitro group), 1273.07 (C–N str., coupled vibrations amide), 841.00 (CH out of plane bending, 4-substituted pyridine), 739.73 (OCN deformations, amide IV band), 667.40 (OCN deformations, amide VI band).

Evaluation of antimycobacterial activity

All compounds were screened for their in vitro antimycobacterial activity against MTB, in Middlebrook 7H11agar medium supplemented with OADC by agar dilution method similar to that recommended by the National Committee for Clinical Laboratory Standards for the determination of MIC in triplicate (1995). The minimum inhibitory concentration (MIC) is defined as the minimum concentration of compound required to give complete inhibition of bacterial growth.

Evaluation of antimicrobial activity (determination of minimum inhibitory concentration)

The antimicrobial activity was performed against Gram-positive bacteria: *Staphylococcus aureus* and *Bacillus subtilis*, Gram-negative bacterium: *Escherichia coli* and fungal strains: *Candida albicans* and *Aspergillus niger* by tube dilution method (Cappucino and Sherman, 1999). Dilutions of test and standard compounds [norfloxacin (antibacterial) and fluconazole (antifungal)] were prepared in double strength nutrient broth I.P. (bacteria) and Sabouraud dextrose broth I.P. (Pharmacopoeia of India, 2007) (fungi). The samples were incubated at 37°C for 24 h (bacteria), at 25°C for 7 days (*A. niger*), and at 37°C for 48 h (*C. albicans*), and the results were recorded in terms of MIC (the lowest concentration of test substance which inhibited the growth of microorganisms).

QSAR studies

The structures of isonicotinyl hydrazide derivatives were first pre-optimized with the Molecular Mechanics Force Field (MM+) procedure included in Hyperchem 6.03 (1993) and the resulting geometries are further refined by means of the semiempirical method PM3 (Parametric Method-3). We chose a gradient norm limit of 0.01 kcal/Å for the geometry optimization. The lowest energy structure was used for each molecule to calculate physicochemical properties using TSAR 3.3 software for Windows (TSAR 3D Version 3.3, 2000). Further, the regression analysis was performed using the SPSS software package (1999). The predictive powers of the equation were validated by determination of cross-validated $r^2$ ($q^2$) using leave one out (LOO) cross-validation method (Schaper, 1999).

Calculation of statistical parameters

The developed QSAR models were validated by the calculation of following statistical parameters : probable error of the coefficient of correlation (PE), least square error (LSE), Friedman's lack of fit measure (LOF), standard error of prediction ($SE_P$), quality value ($Q$), and sum of squares of response values (SSY) (Mandloi *et al*., 2005; Pinheiro *et al*., 2004].

These parameters were calculated from the following equations:

$$PE = 2\left(1 - r^2\right)/3\sqrt{n}$$

where $r$ is the correlation coefficient and $n$ is the number of compounds used.

$$LSE = \Sigma\left(Y_{obs} - Y_{calc}\right)^2$$

where $Y_{obs}$ and $Y_{calc}$ are the observed and calculated values, respectively.

$$LOF = LSE/\{1 - (C + d \cdot p/n)\}^2$$

where LSE is the least square error, $C$ is the number of descriptors +1, $p$ is the number of independent parameters,

$n$ is the number of compounds used, $d$ is the smoothing parameter which controls the bias in the scoring factor between equations with different number of terms and was kept 1.0.

$$SE_P = \sqrt{LSE/n}$$

The quality value, $Q$, is given by

$$Q = r/SE$$

where $Q$ is the quality value, $r$ is the correlation coefficient, and SE is the standard error.

The predictive ability of QSAR models was also quantified in terms of $q^2$, which is defined as

$$q^2 = 1 - \left\{ \Sigma (Y_{obs} - Y_{calc})^2 \Big/ \Sigma (Y_{obs} - Y_{mean})^2 \right\}$$

The low value of PE, LSE, LOF, and $SE_P$ and high value of $Q$ and $q^2$ are the essential criteria for qualifying the model as the best one.

### Evaluation of anti-HIV activity

The anti-HIV activity and cytotoxicity were evaluated against HIV-1 strain IIIB and HIV-2 ROD in MT-4 cell cultures using the 3-(4,5-dimethylthiazol-2-yl)-2,5-diphenyltetrazolium bromide (MTT) method (Pauwels *et al.*, 1988). Briefly, virus stocks were titrated in MT-4 cells and expressed as the 50% cell culture infective dose ($CCID_{50}$). MT-4 cells were suspended in culture medium at $1 \times 10^5$ cells/ml and infected with HIV at a multiplicity of infection of 0.02. Immediately after viral infection, 100 µl of the cell suspension was placed in each well of a flat-bottomed microtiter tray containing various concentrations of the test compounds. After a 4-day incubation period at 37°C, the number of viable cells was determined using the MTT method. Compounds were tested in parallel for cytotoxic effects in uninfected MT-4 cells.

### Antiviral assays

The antiviral assays [except anti-human immunodeficiency virus (HIV) assays] were based on inhibition of virus-induced cytopathicity in HEL [herpes simplex virus type 1 (HSV-1), HSV-2 (G), vaccinia virus, and vesicular stomatitis virus], Vero (parainfluenza-3, reovirus-1, Sindbis, Coxsackie B4, and Punta Toro virus), HeLa (vesicular stomatitis virus, Coxsackie virus B4, and respiratory syncytial virus) cell cultures. Confluent cell cultures in microtiter 96-well plates were inoculated with 100 cell culture inhibitory dose-50 ($CCID_{50}$) of virus (1 $CCID_{50}$ being the virus dose to infect 50% of the cell cultures) in the presence of varying concentrations (100, 20, 4, … µg/ml) of the test compounds. Viral cytopathicity was recorded as soon as it reached completion in the control virus-infected cell cultures that were not treated with the test compounds.

## Results and discussion

### Chemistry

The synthesis of target compounds was carried out as depicted in Scheme 1. The isonicotinic acid was refluxed with ethanol in the presence of sulfuric acid to get the ethyl ester of isonicotinic acid. The ester thus obtained was refluxed with hydrazine hydrate to obtain the isonicotinic acid hydrazide. The isonicotinic acid hydrazide was refluxed with various substituted aldehydes to yield the target hydrazones (**1**–**9**, **15**). Furthermore, the reaction of compounds **1**–**3**, **5**, **6**, and **15** with benzoyl chloride, which was prepared by refluxing benzoic acid with thionyl chloride, resulted in the formation of benzoylated derivatives **10**–**14**, **16**. All the compounds were obtained in appreciable yield and their physicochemical characteristics are presented in Table 1.

The structures of synthesized compounds were ascertained on the basis of their consistent IR an NMR spectral characteristics. The presence of singlet signal above $\delta$ 11.50 ppm in compounds **1**, **2**, **3**, **4**, **5**, **6**, **7**, **8**, and **9** reveals the presence of the proton NH and it disappears in the compounds **10**, **11**, **12**, **13**, **14**, and **16**.

The presence of singlet signal around $\delta$ 8.0 ppm confirms the presence of N=CH linkage in the synthesized compounds. In all the synthesized compounds two doublet signals were observed at two different $\delta$ values, with the one at higher $\delta$ value corresponds to $C_2$ and $C_6$ CH protons as they are in close proximity of the electronegative nitrogen atom in the ring and the doublet signal at lower $\delta$ represents the remaining two protons of the isonicotinyl nucleus. The singlet signal due to NH at $\delta$ 11.24 ppm in compound **8** confirms the presence of the indole nucleus in the synthesized compounds. The appearance of multiplet signals in the aromatic region in compounds **10**, **12**, and **14** confirmed the existence of an acyl group in these compounds. The singlet signal at $\delta$ 3.28 ppm confirms the presence of a methyl group in compound **5**. The singlet signal at $\delta$ 3.36 ppm confirms the presence of a 3,4,5-trimethoxy group in compound **4**. The presence of $CH_3$ group in compound **5** was depicted by the singlet signal at $\delta$ 3.28 ppm. The singlet signal at $\delta$ 2.48 ppm corresponding to the $SCH_3$ group confirms the presence of thiomethyl group in compound **12**.

The presence of the C=O functional group was marked by the appearance of stretching band around 1680–1640 $cm^{-1}$, in compounds **1**, **4**, **5**, and **8** which is

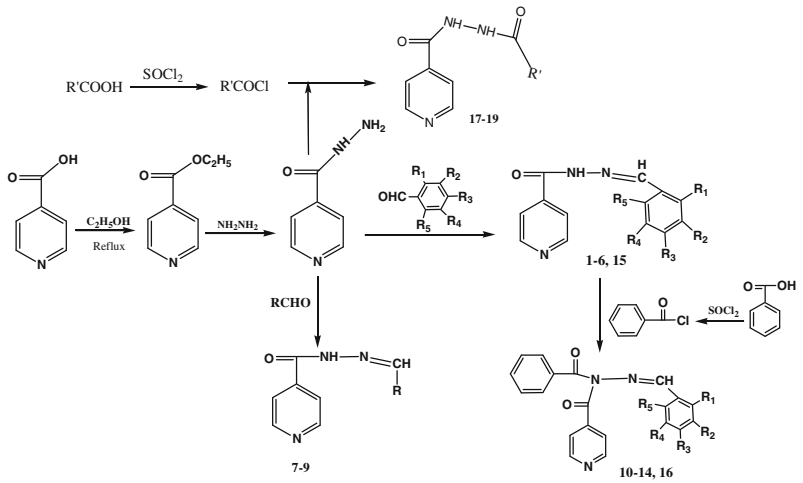


| Comp. | $R_1$ | $R_2$ | $R_3$ | $R_4$ | $R_5$ | R | R' |
|---|---|---|---|---|---|---|---|
| **1** | H | $OC_2H_5$ | OH | H | H | - | - |
| **2** | H | $OCH_3$ | OH | H | H | - | - |
| **3** | $OCH_3$ | H | H | H | $OCH_3$ | - | - |
| **4** | H | $OCH_3$ | $OCH_3$ | $OCH_3$ | H | - | - |
| **5** | H | H | $CH_3$ | H | H | - | - |
| **6** | H | H | $SCH_3$ | H | H | - | - |
| **7** | - | - | - | - | - |  | - |
| **8** | - | - | - | - | - |  | - |
| **9** | - | - | - | - | - |  | - |
| **10** | H | $OCH_3$ | OH | H | H | - | - |
| **11** | H | $OC_2H_5$ | OH | H | H | - | - |
| **12** | H | H | $SCH_3$ | H | H | - | - |
| **13** | $OCH_3$ | H | H | H | $OCH_3$ | - | - |
| **14** | H | H | $CH_3$ | H | H | - | - |
| **15** | OH | H | H | H | H | - | - |
| **16** | OH | H | H | H | H | - | - |
| **17** | - | - | - | - | - | - | 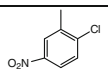 |
| **18** | - | - | - | - | - | - | 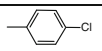 |
| **19** | - | - | - | - | - | - |  |

**Scheme 1** Synthetic route followed for the synthesis of isoniazid derivatives

**Table 1** Physicochemical properties and antimycobacterial activity of synthesized isoniazid derivatives

| Compound | Mol. formula | Mol. wt. | Melting pt. (°C) | Rf[a] | % yield | MIC MTB-H37Rv ($\mu M \times 10^{-3}$) |
|---|---|---|---|---|---|---|
| Training set | | | | | | |
| **1** | $C_{15}H_{15}N_3O_3$ | 285 | Above 242 | 0.78 | 65.3 | 11 |
| **2** | $C_{14}H_{13}N_3O_3$ | 271 | 238–241 | 0.74 | 71.2 | 12 |
| **3** | $C_{15}H_{15}N_3O_3$ | 285 | 193–196 | 0.69 | 68.5 | 11 |
| **4** | $C_{16}H_{17}N_3O_4$ | 315 | 205–208 | 0.71 | 80.7 | 20 |
| **5** | $C_{14}H_{13}N_3O$ | 239 | 198–201 | 0.68 | 84.6 | 52 |
| **6** | $C_{14}H_{13}N_3OS$ | 271 | 175–178 | 0.57 | 71.5 | 12 |
| **7** | $C_{17}H_{13}N_3O_2$ | 291 | 239–242 | 0.59 | 56.8 | 21 |
| **8** | $C_{15}H_{12}N_4O$ | 264 | 225–228 | 0.64 | 61.9 | 24 |
| **9** | $C_{10}H_{11}N_3O$ | 189 | 187–190 | 0.52 | 74.5 | 17 |
| **10** | $C_{21}H_{17}N_3O_4$ | 375 | 230–233 | 0.45 | 57.8 | >67 |
| **11** | $C_{22}H_{19}N_3O_4$ | 389 | 234–237 | 0.43 | 60.4 | >64 |
| **12** | $C_{21}H_{17}N_3O_2S$ | 375 | 226–229 | 0.40 | 45.8 | >67 |
| **13** | $C_{22}H_{19}N_3O_4$ | 389 | 215–218 | 0.51 | 63.9 | >64 |
| **14** | $C_{21}H_{17}N_3O_2$ | 343 | 220–223 | 0.44 | 62.7 | >73 |
| Test set | | | | | | |
| **15** | $C_{13}H_{11}N_3O_2$ | 241 | 230–233 | 0.65 | 50.60 | 52 |
| **16** | $C_{20}H_{15}N_3O_3$ | 345 | 214–217 | 0.48 | 52.4 | >72 |
| **17** | $C_{13}H_9N_4O_4Cl$ | 320 | 200–203 | 0.71 | 56.30 | 4.9 |
| **18** | $C_{13}H_{10}N_3O_2Cl$ | 275 | 216–219 | 0.63 | 71.40 | 22.7 |
| **19** | $C_9H_{10}N_3O_2Cl$ | 227 | 235–238 | 0.69 | 51.80 | 55.1 |
| INH | | | | | | 2.04 |
| ETB[b] | | | | | | 15.31 |
| CFL | | | | | | 9.4 |
| RIF[b] | | | | | | 0.24 |

[a] Mobile phase: ethanol

[b] Sriram *et al*. (2007)

characteristic of the amide linkage. The vibrational frequency C=O functional group shifts to a lower frequency around 1597–1593 $cm^{-1}$, in compounds **10**, **12**, and **14**, which may be due to substitution of NH proton with acyl group. The NH stretching of secondary amide was observed around 3200–3100 $cm^{-1}$ in compounds **1**, **4**, **5**, and **8** and this characteristic peak disappeared in the spectra of compounds **10**, **12**, and **14**. The presence of peaks slightly above and below 3000 $cm^{-1}$ indicates the presence of an aromatic and aliphatic portion in the synthesized compounds, respectively. The skeletal C=C-stretching bands were observed around 1500 $cm^{-1}$ in the spectra of the synthesized compounds which represents the presence of aromatic groups. In compounds **1**, **4**, and **5** the C-O–C stretching was observed at 1276.12, 1248.96, and 1240.0 $cm^{-1}$, which reveals the presence of a methoxy group in their structure. The CH out of plane bending observed around vibrational frequency of 860–814 $cm^{-1}$ indicated the presence of the 4-substituted pyridine ring in the structure of the synthesized compounds.

## Antimycobacterial activity

The in vitro antitubercular activity of synthesized compounds against *M. tuberculosis* (MTB) was carried out in Middlebrook 7H11agar medium supplemented with OADC by agar dilution method and the results are presented in Table 1. The results of antitubercular activity indicated that the synthesized derivatives were active against *M. tuberculosis* (MTB) with an MIC of $11 \times 10^{-3}$ μM which approaches the antitubercular potential of ciprofloxacin. The antimycobacterial potential of compounds **1**, **2**, **3**, and **6** was found to be better than standard drug ethambutol (ETB). It was observed from the results of antimycobacterial activity that compounds with free OH group at *para* position (compounds **1** and **2**) in their molecular structure were more active as compared to other derivatives which may be due the fact that free OH group may be involved in the binding of the drug with the receptor site of the *Mycobacterium*. It can also be seen from the antimycobacterial activity data that when we replaced the OH group with electron donating $CH_3$

group (compound **5**), a fall in activity was observed ($52 \times 10^{-3}$ μM) but if we substituted the $CH_3$ group with $SCH_3$ group (compound **6**), an abrupt rise in activity was observed ($12 \times 10^{-3}$ μM). This may be attributed to the fact that, similar to the binding of the OH group with the target site, $SCH_3$ group containing free lone pair of electrons was involved in the binding of structure with the target site. The substitution of phenyl ring of the aldehydes with naphthalene nucleus (compound **7**) showed antimycobacterial potential but the replacement of the naphthalene with the heterocyclic indole nucleus (compound **8**) leads to a fall in antitubercular activity of the synthesized isoniazid derivatives. The substitution of NH proton of hydrazide with acyl group, $C_6H_5CO$, leads to decrease in antimycobacterial activity of synthesized derivatives (compounds **10**, **11**, **12**, **13**, and **14**) which shows that the NH proton is necessary for antimycobacterial activity.

The test set compounds **15–19** were also evaluated for their antimycobacterial activity and compound **17** was highly active antimycobacterial agent with MIC value $4.9 \times 10^{-3}$ μM and was twice active than ciprofloxacin and thrice active than ethambutol.

From the results of antimycobacterial activity the following conclusions regarding structure activity relationship (SAR) can be drawn:

1. From the appreciable antimycobacterial activity of compounds **1** and **2** it may be concluded that the presence of a free hydroxyl group at *para* position, OH, is necessary for antimycobacterial activity.
2. The substitution of the OH group with an electron donating $CH_3$ (compound **5**) decreases the antimycobacterial activity. These results are similar to the reports of Sriram *et al.* (2007) who observed that the addition of a methyl group decreases the antimycobacterial activity of *N*-hydroxythiosemicarbazones.
3. The replacement of the benzylidene ring with a naphthalene ring (compound **7**) or a heterocyclic indole ring (compound **8**) did not improve the antimycobacterial activity. This is similar to one of our previous reports (Kumar *et al.*, 2009).
4. The presence of the OH group at *ortho* position (compound **7**) increases the activity of the compounds. This is in concordance with Tripathi *et al.* (2006) who stated that the OH group at *ortho* position leads to a measurable change in activity of the compounds.
5. The substitution of the methyl group (compound **5**) with the more bulky thiomethyl group (compound **6**) increased the antimycobacterial activity. This is in accordance with the results of Desai *et al.* (2001) who reported that addition of a bulkier group at the 4-position positively contributes to the antimycobacterial activity.
6. The presence of electron withdrawing $NO_2$ and Cl groups in the molecular structure (compound **17**) leads to a steep increase in antimycobacterial activity.

## Cytostatic, cytotoxic, and antiviral activities

The compounds were in general poorly cytotoxic against HEL, HeLa, and Vero cell cultures (except **7** that showed an MCC of ≥20 μg/ml for HEL, but 0.2 to ≥0.8 μg/ml for HeLa and Vero cell cultures). Instead, their cytostatic activities ranged between 0.10 μg/ml (compound **7**) and ≥100 μg/ml depending the nature of the compounds (Table 2). Generally, none of the compounds were inhibitory to HIV (Table 2) or any of the other RNA or DNA viruses tested at subtoxic concentrations. Compound **7** showed anti-HSV-1, -HSV-2, and -VV activity at $EC_{50}$ values of 0.06–0.4 μg/ml (Table 3), but given the potent cytostatic activity of this compound, it is unclear whether this represents a direct antiviral effect or, more likely, an

**Table 2** Anti-HIV potential of synthesized isoniazid derivatives in MT-4 cells

| Compound | $EC_{50}$ (μg/ml) | | $CC^{a}_{50}$ (μg/ml) |
|---|---|---|---|
| | HIV-1 (IIIb) | HIV-2 (ROD) | |
| **1** | >102 | >102 | 102 ± 20 |
| **2** | >89 | >89 | ≥89 |
| **3** | >9 | >9 | 9 ± 4.5 |
| **4** | >110 | >110 | 110 ± 12 |
| **5** | >25 | >25 | 25 ± 9 |
| **6** | >59 | >59 | 59 ± 8 |
| **7** | >0.10 | >0.10 | 0.10 ± 0.01 |
| **8** | >95 | >95 | 95 ± 16 |
| **9** | >11 | >11 | 11 ± 10 |
| **10** | >105 | >105 | 105 ± 18 |
| **11** | >92 | >92 | ≥92 |
| **12** | >69 | >69 | 69 ± 8 |
| **13** | >12 | >12 | 12 ± 0.9 |
| **14** | >42 | >42 | 42 ± 11 |
| **15** | >2.52 | >2.52 | 2.52 ± 0.10 |
| **16** | NT | NT | – |
| **17** | >115.67 | >115.67 | 115.67 ± 6.03 |
| **18** | >120.00 | >120.00 | >120.00 |
| **19** | >77.47 | >77.47 | 77.47 ± 58.50 |
| Nevirapine | 0.050 ± 0.011 | >4.0 | >4.0 |
| Zidovudine | 0.002 ± 0.001 | 0.002 ± 0.001 | >25 |

50% Effective concentration or compound concentration required to inhibit virus-induced cytopathicity by 50%

*NT* not tested

[a] 50% Cytotoxic concentration or compound concentration required to reduce MT-4 cell viability by 50%

**Table 3** Cytotoxicity and anti-DNA virus activity of synthesized isoniazid derivatives in HEL cell cultures

| Compound | Minimum cytotoxic concentration[a] (μg/ml) | $EC_{50}$[b] (μg/ml) | | | |
|---|---|---|---|---|---|
| | | Herpes simplex virus-1 (KOS) | Herpes simplex virus-2 (G) | Vaccinia virus | Herpes simplex virus-1 $TK^-$ KOS $ACV^r$ |
| **1** | >100 | >100 | >100 | >100 | >100 |
| **2** | >100 | >100 | >100 | >100 | >100 |
| **3** | >100 | >100 | >100 | >100 | >100 |
| **4** | >100 | >100 | >100 | >100 | >100 |
| **5** | >100 | >100 | >100 | >100 | >100 |
| **6** | >100 | >100 | >100 | >100 | >100 |
| **7** | ≥20 | 0.06 | 0.4 | 0.14 | 0.4 |
| **8** | >100 | >100 | >100 | >100 | >100 |
| **9** | 100 | >20 | >20 | >20 | >20 |
| **10** | >100 | >100 | >100 | >100 | >100 |
| **11** | >100 | >100 | >100 | >100 | >100 |
| **12** | >100 | >100 | >100 | >100 | >100 |
| **13** | >100 | >100 | >100 | >100 | >100 |
| **14** | >100 | >100 | >100 | >100 | >100 |

[a] Required to cause a microscopically detectable alteration of normal cell morphology

[b] Required to reduce virus-induced cytopathicity by 50%

**Table 4** Cytotoxicity and anti-RNA virus activity of synthesized isoniazid derivatives in HeLa cell cultures

| Compound | Minimum cytotoxic concentration[a] (μg/ml) | $EC_{50}$[b] (μg/ml) | | |
|---|---|---|---|---|
| | | Vesicular stomatitis virus | Coxsackie virus B4 | Respiratory syncytial virus |
| **1** | >100 | >100 | >100 | >100 |
| **2** | 100 | >20 | >20 | >20 |
| **3** | 100 | >20 | >20 | >20 |
| **4** | ≥100 | >100 | >100 | >100 |
| **5** | 100 | >20 | 9 | >20 |
| **6** | 100 | >20 | >20 | >20 |
| **7** | 0.2 | >0.04 | >0.04 | >0.04 |
| **8** | ≥100 | >100 | >100 | >100 |
| **9** | 100 | >20 | >20 | >20 |
| **10** | 100 | >20 | >20 | >20 |
| **11** | >100 | >100 | >100 | >100 |
| **12** | >100 | >100 | >100 | >100 |
| **13** | 20 | >4 | >4 | >4 |
| **14** | 100 | >20 | >20 | >20 |

[a] Required to cause a microscopically detectable alteration of normal cell morphology

[b] Required to reduce virus-induced cytopathicity by 50%

indirect cytostatic effect of the compound. Compounds **5**, **6**, **7**, and **12** were found to be inhibitory to Coxsackie B4 virus in one cell line but not in another (Tables 4, 5). Instead, compound **8** showed an $EC_{50}$ of 2.4 μg/ml against reovirus-1 in Vero cell cultures that is at a concentration well below its toxicity threshold. This observed activity is further under investigation.

## Antibacterial and antifungal activities

The synthesized isoniazid derivatives (**1**–**19**) were evaluated in vitro for their antibacterial activity against Gram-positive *S. aureus*, *B. subtilis*, Gram negative *E. coli* and antifungal activity against *C. albicans* and *A. niger* by the serial dilution method (Cappucino and Sherman, 1999) using norfloxacin and fluconazole as reference standards for antibacterial and antifungal activities, respectively, and the results are presented in Table 6.

For antibacterial activity against *B. subtilis* all the synthesized derivatives were more active than the isoniazid. In particular, the compounds **4** and **13** were found to be the most effective antibacterial agents having $pMIC_{bs}$ values 2.40 and 2.49 μM, respectively. The antibacterial activity value of these compounds approaches the antibacterial potential of

**Table 5** Cytotoxicity and anti-RNA virus activity of synthesized isoniazid derivatives in Vero cell cultures

| Compound | Minimum cytotoxic concentration[a] (μg/ml) | $EC_{50}^{b}$ (μg/ml) | | | | |
|---|---|---|---|---|---|---|
| | | Para influenza-3 virus | Reovirus-1 | Sindbis virus | Coxsackie virus B4 | Punta Toro virus |
| **1** | >100 | >100 | >100 | >100 | >100 | >100 |
| **2** | >100 | >100 | >100 | >100 | >100 | >100 |
| **3** | 100 | >20 | >20 | >20 | >20 | >20 |
| **4** | >100 | >100 | >100 | >100 | >100 | >100 |
| **5** | ≥20 | >20 | >20 | >20 | >20 | >20 |
| **6** | ≥100 | >100 | >100 | >100 | 9 | >100 |
| **7** | ≥0.8 | >0.8 | >0.8 | >0.8 | >0.8 | >0.8 |
| **8** | >100 | >100 | 2.4 | >100 | 45 | >100 |
| **9** | 100 | >20 | >20 | >20 | >20 | >20 |
| **10** | ≥100 | >100 | >100 | >100 | >100 | >100 |
| **11** | >100 | >100 | >100 | >100 | >100 | >100 |
| **12** | ≥100 | >100 | >100 | >100 | 9 | >100 |
| **13** | 100 | >20 | >20 | >20 | >20 | >20 |
| **14** | ≥20 | >20 | >20 | >20 | >20 | >20 |

[a] Required to cause a microscopically detectable alteration of normal cell morphology

[b] Required to reduce virus-induced cytopathicity by 50%

**Table 6** Antibacterial and antifungal potentials (μM/ml) of synthesized isoniazid derivatives

| Compound | $pMIC_{bs}$ | $pMIC_{sa}$ | $pMIC_{ec}$ | $pMIC_{ca}$ | $pMIC_{an}$ | $pMIC_{b}$ | $pMIC_{f}$ | $pMIC_{am}$ |
|---|---|---|---|---|---|---|---|---|
| Training set | | | | | | | | |
| **1** | 2.06 | 2.06 | 2.36 | 2.36 | 2.36 | 2.16 | 2.36 | 2.24 |
| **2** | 2.04 | 2.04 | 2.34 | 2.34 | 2.34 | 2.14 | 2.34 | 2.22 |
| **3** | 2.06 | 2.06 | 2.06 | 2.36 | 2.36 | 2.06 | 2.36 | 2.18 |
| **4** | 2.40 | 2.10 | 2.10 | 2.40 | 2.40 | 2.20 | 2.40 | 2.28 |
| **5** | 1.98 | 1.98 | 1.98 | 2.28 | 2.28 | 1.98 | 2.28 | 2.1 |
| **6** | 2.04 | 2.04 | 2.34 | 2.34 | 2.34 | 2.14 | 2.34 | 2.22 |
| **7** | 2.07 | 2.07 | 2.07 | 2.37 | 2.37 | 2.07 | 2.37 | 2.19 |
| **8** | 2.02 | 2.02 | 2.02 | 2.63 | 2.32 | 2.02 | 2.48 | 2.2 |
| **9** | 1.88 | 1.88 | 1.88 | 2.48 | 2.18 | 1.88 | 2.33 | 2.06 |
| **10** | 2.18 | 2.48 | 2.48 | 3.08 | 2.48 | 2.38 | 2.78 | 2.54 |
| **11** | 2.19 | 2.19 | 2.49 | 2.79 | 2.19 | 2.29 | 2.49 | 2.37 |
| **12** | 2.18 | 2.18 | 2.48 | 2.78 | 2.48 | 2.28 | 2.63 | 2.42 |
| **13** | 2.49 | 2.49 | 2.49 | 3.10 | 2.49 | 2.49 | 2.80 | 2.61 |
| **14** | 2.14 | 2.44 | 2.44 | 2.74 | 2.44 | 2.34 | 2.59 | 2.44 |
| INH | 1.74 | 2.04 | 1.74 | 2.34 | 2.04 | 1.84 | 2.19 | 1.98 |
| SD | 0.18 | 0.19 | 0.25 | 0.28 | 0.13 | 0.18 | 0.18 | 0.18 |
| Test set | | | | | | | | |
| **15** | 1.98 | 1.98 | 2.29 | 2.29 | 2.29 | 2.08 | 2.29 | 2.17 |
| **16** | 2.44 | 1.84 | 2.44 | 3.04 | 2.44 | 2.24 | 2.74 | 2.44 |
| **17** | 2.11 | 2.11 | 2.11 | 2.41 | 2.41 | 2.11 | 2.41 | 2.23 |
| **18** | 2.34 | 2.34 | 1.74 | 2.64 | 1.74 | 2.14 | 2.19 | 2.16 |
| **19** | 1.96 | 2.26 | 2.26 | 2.26 | 2.26 | 2.16 | 2.26 | 2.20 |
| Std. | 2.61[a] | 2.61[a] | 2.61[a] | 2.64[b] | 2.64[b] | 2.61 | 2.64 | 2.62 |

*SD* standard deviation

[a] Norfloxacin, [b] Fluconazole

the standard drug norfloxacin. In case of *S. aureus*, compounds **10** and **13** have shown marked antibacterial potential at $pMIC_{sa}$ values 2.48 and 2.49 μM, respectively. For antibacterial activity against *E. coli* compounds **10–13** had shown better antibacterial activity with $pMIC_{ec}$ values of 2.48, 2.49, 2.48, and 2.49 μM, respectively.

The antifungal activity against *C. albicans* revealed that compounds **10** and **13** were the potential candidates having $pMIC_{ca}$ values 3.08 and 3.10 μM, respectively. The compounds **10** and **13** have better antifungal activity than the standard drug fluconazole. In case of *A. niger* compounds **10**, **12**, and **13** were found to be active with $pMIC_{an}$ values 2.48, 2.48, and 2.49 μM, respectively.

The test set compounds (**15–19**) were also active against the tested microorganisms and compounds **16** and **18** were the most active among them, with their antifungal activity against *C. albicans* better than the standard drug fluconazole.

It can be observed from the results presented in Table 6 that the synthesized isoniazid derivatives have higher antifungal potential particularly against *C. albicans*. The compounds were also found to be more active against Gram-negative *E. coli* as compared to Gram-positive *B. subtilis* and *S. aureus*.

## Structure activity relationship

From the results of antimicrobial activity, the following structure activity the relationship can be drawn:

1. The compounds have shown marked antifungal potential as compared to antibacterial activity, which shows that there are different structural requirements are essential for antibacterial and antifungal activities. These results are similar to those of Sortino *et al.* (2007).
2. It can also be seen from the results of antibacterial and antifungal activities that the activity increases with the addition of a bulkier substituent on the phenyl nucleus of the synthesized compounds which can be easily seen from the higher activity of compound **1** in comparison to compounds **2** and **6** in comparison to compound **5**, respectively.
3. The results of antimicrobial activity depicted that the presence of electron donating group, $OCH_3$, enhanced the antimicrobial activity of the synthesized derivatives. It can be observed from the results of antimicrobial activity that compound **2** was active and the addition of $OCH_3$ group made it more active (compound **3**) and further addition of $OCH_3$ (compound **4**) made the structure of the molecule highly active against the tested strains. This is supported by results of Emami *et al.* (2008).
4. The synthesized derivatives were more active toward the Gram-negative bacterium *E. coli* than Gram-positive *B. subtilis* and *S. aureus*. This finding is in agreement with Sbardella *et al.* (2004).
5. The substitution of NH proton with acyl group (compounds **10–14**) leads to increase in activity of the compounds. This may be due to the increase in lipophilicity of the molecules which may allow them to easily penetrate the microbial membrane. These results are in agreement with the observations of Imramovsky *et al.* (2007). These results are in contrast with the results of antimycobacterial activity where the activity decreases due to the $N_1$-benzoylation.
6. The presence of substituent at *ortho* position increases the antibacterial and antifungal potentials of the compounds which can be seen from the antimicrobial activity of compounds **3**, **7**, and **13**. This fact is supported by the observations of Guven *et al.* (2007).
7. Compound **17** was found to be highly active which may be due to the presence of electron withdrawing groups $NO_2$ and Cl in its structure.
8. Compound **16** having OH group at *ortho* position and NH proton being replaced by benzoyl group was also found to be highly active that may be attributed to the free OH group and its increased lipophilicity.

The SAR findings of the antimycobacterial and antimicrobial activities are summarized in Fig. 1.

## QSAR studies

### *Development of one-target QSAR model*

In order to identify the substituent effect on the antimicrobial activity, quantitative structure activity relationship (QSAR) studies between the in vitro activity and descriptors coding for lipophilic, electronic, steric, and topological properties of the 14 synthesized isoniazid derivatives (training set) were undertaken, using the linear free energy relationship model (LFER) described by Hansch and Fujita (1964). Biological activity data determined as MIC values were first transformed into pMIC values (i.e., −log MIC) and used as dependent variable in QSAR study. The different molecular descriptors (independent variables) like log of octanol–water partition coefficient (log P), molar refractivity (MR), Kier's molecular connectivity ($^0\chi$, $^0\chi^v$, $^1\chi$, $^1\chi^v$, $^2\chi$, $^2\chi^v$) and shape ($\kappa_1$, $\kappa_2$, $\kappa_3$, $\kappa\alpha_1$, $\kappa\alpha_2$, $\kappa\alpha_3$) topological indices, Randic topological index ($R$), Balaban topological index ($J$), Wiener topological index ($W$), total energy ($T_e$), energies of highest occupied molecular orbital (HOMO) and lowest unoccupied molecular orbital (LUMO), dipole moment ($\mu$), nuclear repulsion energy (Nu.E) and electronic energy (Ele.E), calculated for

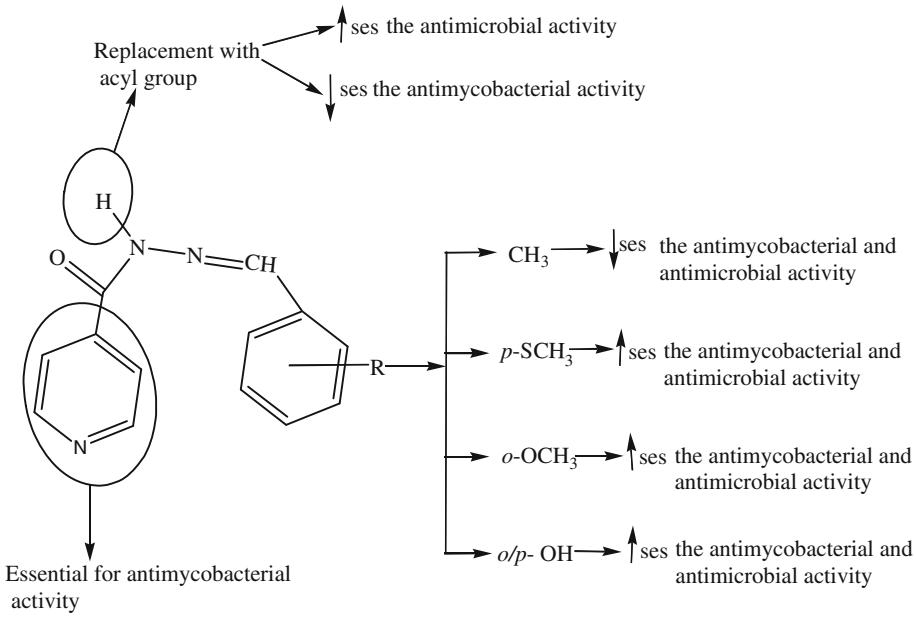


**Fig. 1** Structural requirements for the antimycobacterial and antimicrobial activities of synthesized isoniazid derivatives

isoniazid derivatives are presented in Table 7 (Hansch *et al*., 1973; Kier and Hall, 1976; Randic, 1975, 1993; Balaban, 1982; Wiener, 1947). Units of the energies and dipole were electron volts (eV) and atomic units (a.u.), respectively (Dai *et al*., 1999).

In this study, a data set of 15 compounds (14 isoniazid derivatives along with isoniazid itself) was subjected to linear free energy regression analysis for model generation. Preliminary analysis was carried out in terms of correlation analysis. A correlation matrix constructed for antibacterial activity against *E. coli* is presented in Table 8. The correlations of different molecular descriptors with antibacterial and antifungal activities are presented in Table 9. In general, high colinearity ($r > 0.8$) was observed between different parameters. The high interrelationship was observed between ${}^{0}\chi$ and ${}^{1}\chi$ ($r = 0.998$) and low interrelationship was observed between $T_e$ and $\mu$ ($r = 0.072$). The correlation matrix indicated the predominance of topological parameters and electronic parameters in describing the antimicrobial activity of the synthesized compounds.

The antibacterial activity of synthesized isoniazid derivatives against *E. coli* is governed by the valence first-order molecular connectivity topological index (${}^{1}\chi^{v}$) (Eq. 1).

*ot-QSAR model for antibacterial activity against E. coli*

$$\mathrm{pMIC_{ec}} = 0.123\,{}^{1}\chi^{v} + 1.389 \qquad (1)$$

$$n = 15, \quad r = 0.893, \quad q^2 = 0.756, \quad s = 0.118, \quad F = 50.93.$$

Here and thereafter, $n$ is the number of data points, $r$ is the correlation coefficient, $q^2$ is the cross-validated, $r^2$ is obtained by LOO method, $s$ is the standard error of the estimate, and F is the Fischer statistics.

For antibacterial activity against *E. coli*, the developed QSAR model (Eq. 1) describes the importance of valence first-order molecular connectivity topological index (${}^{1}\chi^{v}$). Topological indices are numerical quantifiers of molecular topology and are sensitive to bonding pattern, symmetry, content of heteroatom as well as degree of complexity of atomic neighborhoods (Lather and Madan, 2005). The valence first-order molecular connectivity topological index (${}^{1}\chi^{v}$) represents the molecules with branched structure. In this case, the positive correlation was observed between ${}^{1}\chi^{v}$ and antibacterial activity against *E. coli* and the results presented in Table 9 are in concordance with the model expressed by Eq. 1 and values of ${}^{1}\chi^{v}$ shown in Table 10 which depict that compounds **10**, **11**, **12**, and **13** having high ${}^{1}\chi^{v}$ values (8.35, 8.93, 9.53, and 8.74) have got the highest antibacterial potential (2.48, 2.49, 2.48, and 2.49).

The QSAR model expressed by Eq. 1 was cross-validated by its high $q^2$ values ($q^2 = 0.756$) obtained with LOO method. The value of $q^2$ greater than 0.5 is the basic requirement for qualifying a QSAR model to be valid one (Golbraikh and Tropsha, 2002). The comparison of observed and predicted antibacterial activities is presented in Table 10. It can be seen from the results that the observed and predicted antibacterial activities lie close to each other as evidenced by their low residual values (Table 10). The plots of observed, predicted, and residual pMIC activity values were also developed to check the statistical validity of QSAR models. The plot of predicted $\mathrm{pMIC_{ec}}$ against observed $\mathrm{pMIC_{ec}}$ (Fig. 2) also favors the model expressed by Eq. 1. Further, the plot of observed $\mathrm{pMIC_{ec}}$ versus residual $\mathrm{pMIC_{ec}}$

**Table 7** Value of selected descriptors used in the regression analysis

| Compound | log *P* | MR | $^{0}\chi$ | $^{0}\chi^{v}$ | $^{1}\chi$ | $^{1}\chi^{v}$ | $^{2}\chi$ | $^{2}\chi^{v}$ | $\kappa_1$ | $\kappa\alpha_1$ | *W* | $T_e$ | Ele.E | LUMO | HOMO | Nu.E |
|---|---|---|---|---|---|---|---|---|---|---|---|---|---|---|---|---|
| **1** | 2.38 | 78.46 | 15.08 | 11.48 | 10.20 | 6.40 | 8.51 | 4.10 | 17.36 | 15.77 | 1100.00 | −3706.88 | −22404.60 | −0.64 | −8.60 | 18697.70 |
| **2** | 2.04 | 73.71 | 14.37 | 10.78 | 9.70 | 5.81 | 8.13 | 3.87 | 16.37 | 14.79 | 956.00 | −3551.09 | −20697.90 | −0.66 | −8.72 | 17146.80 |
| **3** | 2.07 | 78.48 | 15.08 | 11.74 | 10.26 | 6.20 | 8.24 | 4.01 | 17.36 | 15.77 | 1034.00 | −3706.07 | −23220.10 | −0.57 | −8.57 | 19514.10 |
| **4** | 1.82 | 84.95 | 16.66 | 13.07 | 11.19 | 6.73 | 9.05 | 4.39 | 19.33 | 17.70 | 1354.00 | −4181.98 | −26948.80 | −0.72 | −8.74 | 22766.90 |
| **5** | 3.05 | 70.60 | 12.79 | 10.00 | 8.75 | 5.56 | 7.43 | 3.85 | 14.41 | 12.91 | 727.00 | −2910.53 | −16804.60 | −0.62 | −8.84 | 13894.10 |
| **6** | 2.67 | 78.46 | 13.50 | 11.29 | 9.29 | 6.99 | 7.60 | 4.66 | 15.39 | 14.23 | 858.00 | −3104.86 | −18266.70 | −0.64 | −8.10 | 15161.80 |
| **7** | 3.30 | 83.70 | 15.36 | 11.60 | 10.75 | 6.70 | 9.23 | 4.65 | 16.84 | 14.83 | 1155.00 | −3614.56 | −22975.60 | −0.72 | −8.59 | 19361.00 |
| **8** | 2.35 | 76.64 | 13.79 | 10.58 | 9.84 | 6.14 | 8.35 | 4.22 | 14.92 | 13.17 | 927.00 | −3230.67 | −19617.70 | −0.52 | −8.17 | 16387.10 |
| **9** | 1.77 | 55.70 | 10.23 | 7.84 | 6.84 | 4.19 | 5.22 | 2.48 | 12.07 | 11.07 | 363.00 | −2370.69 | −12032.40 | −0.74 | −9.05 | 9661.69 |
| **10** | 3.95 | 103.45 | 19.93 | 15.02 | 13.60 | 8.35 | 11.58 | 5.70 | 22.68 | 20.03 | 2092.00 | −4821.59 | −35250.20 | −0.56 | −8.72 | 30428.60 |
| **11** | 4.30 | 108.20 | 20.64 | 15.73 | 14.10 | 8.93 | 11.96 | 5.93 | 23.66 | 21.00 | 2324.00 | −4977.37 | −37270.20 | −0.55 | −8.68 | 32292.80 |
| **12** | 4.58 | 108.20 | 19.06 | 15.53 | 13.19 | 9.53 | 11.05 | 6.49 | 21.70 | 19.47 | 1930.00 | −4375.34 | −32386.70 | −0.57 | −8.20 | 28011.40 |
| **13** | 3.98 | 108.22 | 20.64 | 15.98 | 14.13 | 8.74 | 11.77 | 5.88 | 23.66 | 21.00 | 2252.00 | −4976.67 | −38088.70 | −0.43 | −8.68 | 33112.00 |
| **14** | 4.96 | 100.34 | 18.36 | 14.24 | 12.65 | 8.09 | 10.88 | 5.68 | 20.73 | 18.16 | 1711.00 | −4181.01 | −30568.50 | −0.54 | −9.01 | 26387.50 |
| INH | 0.02 | 36.93 | 7.40 | 5.24 | 4.84 | 2.75 | 3.78 | 1.71 | 8.10 | 7.25 | 121.00 | −1804.50 | −8006.92 | −0.51 | −10.43 | 6202.42 |
| Test set | | | | | | | | | | | | | | | | |
| **15** | 2.294 | 67.250 | 12.795 | 9.446 | 8.771 | 5.286 | 7.328 | 3.494 | 14.410 | 12.876 | 705.000 | −3075.000 | −17335.400 | −0.677 | −8.727 | 14260.4 |
| **16** | 4.205 | 96.989 | 18.355 | 13.688 | 12.665 | 7.824 | 10.777 | 5.327 | 20.727 | 18.121 | 1673.000 | −4345.680 | −31454.400 | −0.657 | −9.027 | 27108.7 |
| **17** | 2.037 | 77.618 | 16.113 | 11.764 | 10.486 | 6.343 | 9.388 | 4.506 | 18.340 | 16.254 | 1162.000 | −4266.060 | −26128.600 | −1.660 | −10.413 | 21862.50 |
| **18** | 2.083 | 70.294 | 13.665 | 10.578 | 9.165 | 5.838 | 7.950 | 4.123 | 15.390 | 13.745 | 808.000 | −3435.390 | −19870.300 | −0.841 | −9.919 | 16434.900 |
| **19** | 0.781 | 54.563 | 11.259 | 8.846 | 7.109 | 7.109 | 6.174 | 6.174 | 13.067 | 12.171 | 414.000 | −2924.200 | −15111.100 | −0.818 | −10.162 | 12186.900 |

**Table 8** Correlation matrix for antibacterial activity of synthesized isoniazid derivatives against *E. coli*

| | log *P* | $^{0}\chi$ | $^{0}\chi^{v}$ | $^{1}\chi$ | $^{1}\chi^{v}$ | $^{2}\chi$ | $^{2}\chi^{v}$ | $^{3}\chi$ | $\kappa_1$ | *W* | $T_e$ | Ele.E | $\mu$ | Nu.E | $pMIC_{ec}$ |
|---|---|---|---|---|---|---|---|---|---|---|---|---|---|---|---|
| log *P* | 1.000 | | | | | | | | | | | | | | |
| $^{0}\chi$ | 0.851 | 1.000 | | | | | | | | | | | | | |
| $^{0}\chi^{v}$ | 0.863 | 0.992 | 1.000 | | | | | | | | | | | | |
| $^{1}\chi$ | 0.865 | 0.998 | 0.992 | 1.000 | | | | | | | | | | | |
| $^{1}\chi^{v}$ | 0.902 | 0.958 | 0.980 | 0.966 | 1.000 | | | | | | | | | | |
| $^{2}\chi$ | 0.884 | 0.992 | 0.982 | 0.997 | 0.963 | 1.000 | | | | | | | | | |
| $^{2}\chi^{v}$ | 0.921 | 0.949 | 0.969 | 0.960 | 0.995 | 0.963 | 1.000 | | | | | | | | |
| $^{3}\chi$ | 0.853 | 0.970 | 0.949 | 0.970 | 0.920 | 0.981 | 0.928 | 1.000 | | | | | | | |
| $\kappa_1$ | 0.835 | 0.997 | 0.991 | 0.991 | 0.951 | 0.980 | 0.935 | 0.957 | 1.000 | | | | | | |
| *W* | 0.839 | 0.985 | 0.972 | 0.981 | 0.943 | 0.976 | 0.932 | 0.958 | 0.982 | 1.000 | | | | | |
| $T_e$ | −0.778 | −0.991 | −0.976 | −0.985 | −0.923 | −0.974 | −0.906 | −0.959 | −0.992 | −0.975 | 1.000 | | | | |
| Ele.E | −0.820 | −0.992 | −0.978 | −0.987 | −0.937 | −0.978 | −0.924 | −0.959 | −0.991 | −0.995 | 0.988 | 1.000 | | | |
| $\mu$ | −0.306 | −0.137 | −0.189 | −0.132 | −0.256 | −0.125 | −0.271 | −0.125 | −0.141 | −0.229 | 0.072 | 0.189 | 1.000 | | |
| Nu.E | 0.824 | 0.991 | 0.977 | 0.986 | 0.937 | 0.977 | 0.925 | 0.958 | 0.989 | 0.996 | −0.986 | −1.000 | −0.202 | 1.000 | |
| $pMIC_{ec}$ | 0.794 | 0.869 | 0.878 | 0.864 | 0.893 | 0.864 | 0.878 | 0.863 | 0.873 | 0.857 | −0.851 | −0.848 | −0.224 | 0.846 | 1.000 |

**Table 9** Correlation of molecular descriptors with antimicrobial activity of synthesized derivatives

| Mol. descriptor | $pMIC_{bs}$ | $pMIC_{sa}$ | $pMIC_{ec}$ | $pMIC_{ca}$ | $pMIC_{an}$ | $pMIC_{b}$ | $pMIC_{f}$ | $pMIC_{am}$ |
|---|---|---|---|---|---|---|---|---|
| log *P* | 0.573 | 0.682 | 0.794 | 0.676 | 0.655 | 0.784 | 0.754 | 0.798 |
| MR | 0.813 | 0.743 | 0.877 | 0.739 | 0.759 | 0.923 | 0.841 | 0.919 |
| $^{0}\chi$ | 0.847 | 0.773 | 0.869 | 0.750 | 0.737 | 0.941 | 0.842 | 0.931 |
| $^{0}\chi^{v}$ | 0.854 | 0.744 | 0.878 | 0.725 | 0.763 | 0.937 | 0.831 | 0.924 |
| $^{1}\chi$ | 0.837 | 0.767 | 0.864 | 0.752 | 0.746 | 0.933 | 0.846 | 0.928 |
| $^{1}\chi^{v}$ | 0.775 | 0.700 | 0.893 | 0.706 | 0.748 | 0.903 | 0.811 | 0.895 |
| $^{2}\chi$ | 0.808 | 0.771 | 0.864 | 0.747 | 0.739 | 0.925 | 0.840 | 0.920 |
| $^{2}\chi^{v}$ | 0.755 | 0.715 | 0.878 | 0.702 | 0.761 | 0.894 | 0.812 | 0.890 |
| $^{3}\chi$ | 0.780 | 0.798 | 0.863 | 0.706 | 0.708 | 0.924 | 0.796 | 0.903 |
| $^{3}\chi^{v}$ | 0.698 | 0.704 | 0.851 | 0.615 | 0.753 | 0.859 | 0.741 | 0.840 |
| $\kappa_1$ | 0.857 | 0.764 | 0.873 | 0.743 | 0.729 | 0.942 | 0.833 | 0.929 |
| $\kappa_2$ | 0.851 | 0.710 | 0.869 | 0.717 | 0.712 | 0.921 | 0.806 | 0.905 |
| $\kappa\alpha_1$ | 0.867 | 0.739 | 0.876 | 0.718 | 0.734 | 0.939 | 0.815 | 0.920 |
| $\kappa\alpha_2$ | 0.854 | 0.658 | 0.860 | 0.668 | 0.709 | 0.900 | 0.767 | 0.876 |
| *R* | 0.837 | 0.767 | 0.864 | 0.752 | 0.746 | 0.933 | 0.846 | 0.928 |
| *J* | −0.418 | −0.226 | −0.489 | −0.188 | −0.605 | −0.439 | −0.361 | −0.420 |
| *W* | 0.814 | 0.810 | 0.857 | 0.818 | 0.649 | 0.937 | 0.864 | 0.937 |
| $T_e$ | −0.868 | −0.759 | −0.851 | −0.728 | −0.717 | −0.935 | −0.817 | −0.917 |
| Ele.E | −0.846 | −0.812 | −0.848 | −0.798 | −0.688 | −0.944 | −0.862 | −0.941 |
| LUMO | 0.201 | 0.598 | 0.290 | 0.606 | 0.111 | 0.402 | 0.514 | 0.456 |
| HOMO | 0.465 | 0.049 | 0.521 | 0.171 | 0.647 | 0.409 | 0.361 | 0.402 |
| $\mu$ | −0.126 | −0.444 | −0.224 | −0.376 | −0.062 | −0.295 | −0.313 | −0.312 |
| Nu.E | 0.843 | 0.817 | 0.846 | 0.805 | 0.683 | 0.944 | 0.866 | 0.942 |

(Fig. 3) indicated that there was no systemic error in model development as the propagation of error was observed on both sides of zero (Kumar *et al.*, 2007).

Equations 2–5 were developed to predict the antibacterial and antifungal activities of isoniazid derivatives against *B. subtilis*, *S. aureus*, *C. albicans*, and *A. niger*.

**Table 10** Comparison of observed and predicted antibacterial and antifungal activities obtained by ot-QSAR model

| Compound | $pMIC_{ec}$ (Eq. 1) | | | $pMIC_{bs}$ (Eq. 2) | | | $pMIC_{sa}$ (Eq. 3) | | | $pMIC_{ca}$ (Eq. 4) | | | $pMIC_{an}$ (Eq. 5) | | |
|---|---|---|---|---|---|---|---|---|---|---|---|---|---|---|---|
| | Obs | Pre | Res | Obs | Pre | Res | Obs | Pre | Res | Obs | Pre | Res | Obs | Pre | Res |
| **1** | 2.36 | 2.18 | 0.18 | 2.06 | 2.10 | −0.04 | 2.06 | 2.10 | −0.04 | 2.36 | 2.51 | −0.15 | 2.36 | 2.32 | 0.04 |
| **2** | 2.34 | 2.10 | 0.24 | 2.04 | 2.07 | −0.03 | 2.04 | 2.07 | −0.03 | 2.34 | 2.46 | −0.12 | 2.34 | 2.30 | 0.04 |
| **3** | 2.06 | 2.15 | −0.09 | 2.06 | 2.10 | −0.04 | 2.06 | 2.12 | −0.06 | 2.36 | 2.48 | −0.12 | 2.36 | 2.33 | 0.03 |
| **4** | 2.10 | 2.22 | −0.12 | 2.40 | 2.18 | 0.22 | 2.10 | 2.18 | −0.08 | 2.40 | 2.59 | −0.19 | 2.40 | 2.37 | 0.03 |
| **5** | 1.98 | 2.07 | −0.09 | 1.98 | 1.96 | 0.02 | 1.98 | 2.01 | −0.03 | 2.28 | 2.38 | −0.10 | 2.28 | 2.27 | 0.01 |
| **6** | 2.34 | 2.25 | 0.09 | 2.04 | 2.00 | 0.04 | 2.04 | 2.04 | 0.00 | 2.34 | 2.42 | −0.08 | 2.34 | 2.32 | 0.02 |
| **7** | 2.07 | 2.21 | −0.14 | 2.07 | 2.08 | −0.01 | 2.07 | 2.11 | −0.04 | 2.37 | 2.52 | −0.15 | 2.37 | 2.33 | 0.04 |
| **8** | 2.02 | 2.14 | −0.12 | 2.02 | 2.02 | 0.00 | 2.02 | 2.06 | −0.04 | 2.63 | 2.45 | 0.18 | 2.32 | 2.29 | 0.03 |
| **9** | 1.88 | 1.90 | −0.02 | 1.88 | 1.87 | 0.01 | 1.88 | 1.93 | −0.05 | 2.48 | 2.26 | 0.22 | 2.18 | 2.21 | −0.03 |
| **10** | 2.48 | 2.42 | 0.06 | 2.18 | 2.29 | −0.11 | 2.48 | 2.32 | 0.16 | 3.08 | 2.84 | 0.24 | 2.48 | 2.43 | 0.05 |
| **11** | 2.49 | 2.49 | 0.00 | 2.19 | 2.32 | −0.13 | 2.19 | 2.36 | −0.17 | 2.79 | 2.92 | −0.13 | 2.19 | 2.45 | −0.26 |
| **12** | 2.48 | 2.56 | −0.08 | 2.18 | 2.21 | −0.03 | 2.18 | 2.28 | −0.10 | 2.78 | 2.79 | −0.01 | 2.48 | 2.45 | 0.03 |
| **13** | 2.49 | 2.46 | 0.03 | 2.49 | 2.32 | 0.17 | 2.49 | 2.37 | 0.12 | 3.10 | 2.89 | 0.21 | 2.49 | 2.46 | 0.03 |
| **14** | 2.44 | 2.38 | 0.06 | 2.14 | 2.18 | −0.04 | 2.44 | 2.25 | 0.19 | 2.74 | 2.71 | 0.03 | 2.44 | 2.41 | 0.03 |
| INH | 1.74 | 1.73 | 0.01 | 1.74 | 1.77 | −0.03 | 2.04 | 1.87 | 0.17 | 2.34 | 2.18 | 0.16 | 2.04 | 2.13 | −0.09 |
| Test set | | | | | | | | | | | | | | | |
| **15** | 2.29 | 2.04 | 0.25 | 1.98 | 1.98 | 0.00 | 1.98 | 2.02 | −0.04 | 2.29 | 2.37 | −0.08 | 2.29 | 2.26 | 0.03 |
| **16** | 2.44 | 2.35 | 0.09 | 2.44 | 2.20 | 0.24 | 1.84 | 2.27 | −0.43 | 3.04 | 2.72 | 0.32 | 2.44 | 2.39 | 0.05 |
| **17** | 2.11 | 2.17 | −0.06 | 2.11 | 2.18 | −0.07 | 2.11 | 2.16 | −0.05 | 2.41 | 2.53 | −0.12 | 2.41 | 2.33 | 0.08 |
| **18** | 1.74 | 2.11 | −0.37 | 2.34 | 2.04 | 0.30 | 2.34 | 2.06 | 0.28 | 2.64 | 2.41 | 0.23 | 1.74 | 2.29 | −0.55 |
| **19** | 2.26 | 1.97 | 0.29 | 1.96 | 1.96 | 0.00 | 2.26 | 1.98 | 0.28 | 2.26 | 2.28 | −0.02 | 2.26 | 2.24 | 0.02 |

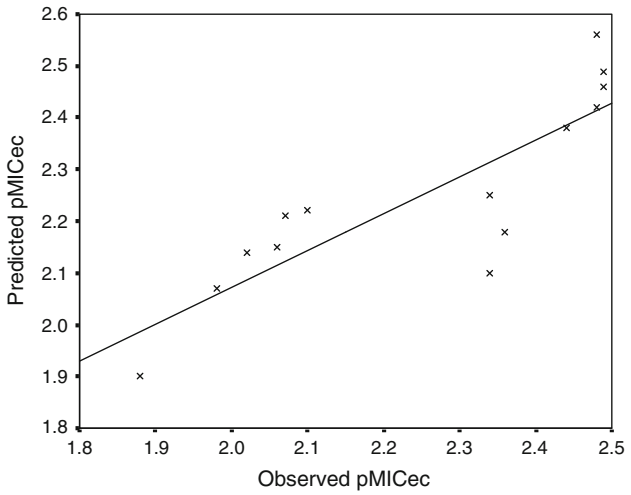


**Fig. 2** Plot of observed pMICec against the predicted pMICec for the linear regression model developed by Eq. 1

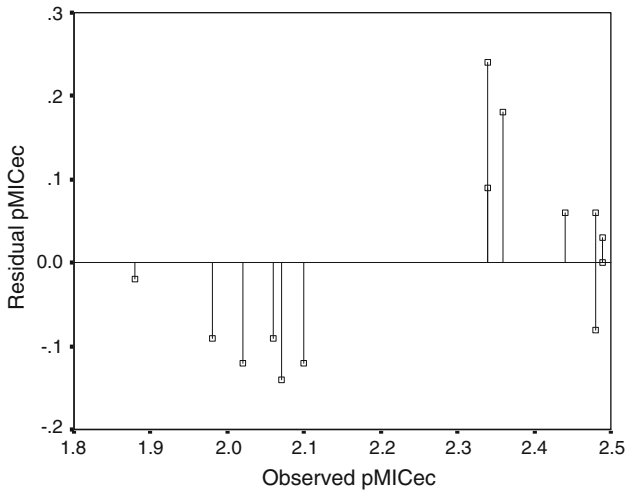


**Fig. 3** Plot of residual pMICec against the experimental pMICec for the linear regression model developed by Eq. 1

*ot-QSAR model for antibacterial activity against B. subtilis*

$$pMIC_{bs} = -0.00017T_e + 1.459 \quad (2)$$

$n = 15, \quad r = 0.868, \quad q^2 = 0.660, \quad s = 0.095, \quad F = 39.79.$

*ot-QSAR model for antibacterial activity against S. aureus*

$$pMIC_{sa} = 0.000019\text{Nu.E} + 1.750 \quad (3)$$

$n = 15, \quad r = 0.817, \quad q^2 = 0.500, \quad s = 0.112, \quad F = 26.05.$

*ot-QSAR model for antifungal activity against C. albicans*

$$\mathrm{pMIC_{ca}} = 0.00034W + 2.134. \quad (4)$$

$n = 15, \quad r = 0.818, \quad q^2 = 0.532, \quad s = 0.165, \quad F = 26.28.$

*ot-QSAR model for antifungal activity against A. niger*

$$\mathrm{pMIC_{an}} = 0.0315\,{}^{0}\chi^{v} + 1.960 \quad (5)$$

$n = 15, \quad r = 0.763, \quad q^2 = 0.351, \quad s = 0.084, \quad F = 18.16.$

The model expressed by Eq. 2 demonstrated that antibacterial activity against *B. subtilis* is governed by the total energy of the molecule ($T_e$). The total energy ($T_e$) calculated by semiempirical methods can be used as a measure of non-specific interactions of the drug with its target site, i.e., the total energies of protonated and neutral molecule, can be considered as a good measure of hydrogen bonds (the higher the energy, the stronger the bond) and can be used to determine the correct localization of the most favorable hydrogen bond acceptor site (Karelson *et al.*, 1996).

As the coefficient of total energy ($T_e$) in Eq. 2 is negative, therefore, the antibacterial activity against *B. subtilis* will increase with decreasing the $T_e$ values. This is clearly evident from Table 6 that compounds **4**, **11**, and **13** having low $T_e$ values −4181.98, −4977.37, and −4976.67 (Table 7) have highest antibacterial activity values of 2.40, 2.19, and 2.49 respectively. Similarly, compounds **5** and **9** having maximum $T_e$ values −2910.53 and −2370.69 (Table 7) have minimum antibacterial activity against *B. subtilis* (Table 6).

In case of *S. aureus*, the developed QSAR model (Eq. 3) indicated the predominance of nuclear repulsion energy in describing the antibacterial activity. The nuclear repulsion energy between two atoms (A and B) is given by

$$E_{\mathrm{Nu.E}}(\mathrm{AB}) = Z_A Z_B / R_{AB}$$

where A is the given atomic species, B is the another atomic species, $Z_A$ is the charge of atomic nucleus A, $Z_B$ is the charge of atomic nucleus B, and $R_{AB}$ is the distance between the atomic nuclei A and B (Clementi, 1980).

The coefficient of nuclear repulsion energy (Nu.E) is positive, which shows that the antibacterial activity will increase with the increase in nuclear repulsion energy of the synthesized compounds, which can be clearly seen from the results of antibacterial activity against *S. aureus* (Table 6) and values of nuclear repulsion energy presented in Table 7 that compounds **10**, **13**, and **14** had the highest antibacterial potential and compounds **5** and **9** had minimal antibacterial activity.

The model described by Eq. 4 depicted the importance of Wiener topological index ($W$) in describing the antifungal activity against *C. albicans*. The Wiener index ($W$) was introduced by Wiener (1947) to demonstrate the correlations between the physicochemical properties of organic compounds and the topological structure of their molecular graphs in terms of sum of distances between any two carbon atoms in the molecule.

The model described by Eq. 5 demonstrated the importance of valence first-order molecular connectivity topological index (${}^{1}\chi^{v}$) in describing the antifungal activity against *A. niger*. The positive correlation of the molecular descriptor with antifungal activity reveals that increase in the value of ${}^{1}\chi^{v}$ (Table 7) will lead to an increase in antifungal activity against *A. niger*. The low residual values presented in Table 10 are in agreement with the fact that models expressed by Eqs. 2–5 are also valid ones.

As in case of Eq. 1, the high $q^2$ values ($q^2 > 0.5$) supported the validity of developed QSAR models described by Eqs. 2–4. The cross-validated correlation coefficient ($q^2 > 0.5$) values obtained for best QSAR model indicated their reliability in predicting the antimicrobial activity of synthesized compounds. In case of *A. niger* the $q^2$ (Eq. 5) value is less than 0.5, which shows that the developed model is an invalid one. But according to the recommendations of Kim *et al.* (2007), the regression models are acceptable if the value of standard deviation (SD, Table 6) is not much larger than 0.3. As the value of standard deviation in case of Eq. 5 is less than 0.3, i.e., 0.28, so the developed model is a valid one. It is important to note that Eqs. 1–5 were derived using the entire data set as there were no outliers in the data set.

Generally for QSAR studies, the biological activities of compounds should span 2–3 orders of magnitude. But in this study, the range of antibacterial and antifungal activities of the synthesized compounds is within one order of magnitude. It is important to note that the predictability of the QSAR models developed in this study is high evidenced by their low residual values. This is in accordance with results suggested by the Bajaj *et al.* (2005), who stated that the reliability of the QSAR model lies in its predictive ability even though the activity data are in the narrow range. Further, recent literature reveals that the QSAR have been applied to describe the relationship between narrow range of biological activity and physicochemical properties of the molecules (Narasimhan *et al.*, 2007; Sharma *et al.*, 2006; Hatya *et al.*, 2006; Kumar *et al.*, 2006). When biological activity data lie in the narrow range, the presence of minimum standard deviation of the biological activity justifies its use in QSAR studies (Kumar *et al.*, 2007; Narasimhan *et al.*, 2007). The minimum standard deviation (Table 6) observed in the antimicrobial activity data justifies its use in QSAR studies. The low value of PE, LSE,

**Table 11** PE, LSE, LOF, $SE_P$, $Q$, $SD_{EP}$, $S_{press}$, $e^-$, and RMSE values calculated for the derived models for modeling antimicrobial activity of synthesized isonicotinic acid-1-(substituted phenyl)-ethylidene/cycloheptylidene hydrazide derivatives

| Equations | Descriptor | PE | LSE | LOF | $SE_P$ | $Q$ | $e^-$ | RMSE | $SD_{EP}$ | $S_{press}$ |
|---|---|---|---|---|---|---|---|---|---|---|
| 1 | $^1\chi^v$ | 0.035 | 0.178 | 0.045 | 0.028 | 7.57 | 0.088 | 0.109 | 0.18 | 0.19 |
| 2 | $T_e$ | 0.042 | 0.116 | 0.029 | 0.023 | 9.14 | 0.061 | 0.088 | 0.09 | 0.16 |
| 3 | Nu.E | 0.057 | 0.163 | 0.041 | 0.027 | 7.30 | 0.085 | 0.104 | 0.11 | 0.15 |
| 4 | $W$ | 0.057 | 0.352 | 0.088 | 0.040 | 4.96 | 0.139 | 0.153 | 0.16 | 0.27 |
| 5 | $^0\chi^v$ | 0.073 | 0.090 | 0.023 | 0.020 | 9.08 | 0.051 | 0.078 | 0.08 | 0.09 |
| 6 | Ele.E | 0.019 | 0.052 | 0.004 | 0.015 | 14.98 | 0.050 | 0.059 | 0.06 | 0.17 |
| 7 | Nu.E | 0.043 | 0.110 | 0.007 | 0.022 | 9.30 | 0.072 | 0.086 | 0.09 | 0.16 |
| 8 | Nu.E | 0.019 | 0.047 | 0.012 | 0.015 | 15.44 | 0.043 | 0.056 | 0.06 | 0.17 |

LOF, standard deviation of prediction ($S_{press}$), and standard deviation error of predictions ($SD_{EP}$) and $SE_P$ and high value of $r^2$ and $Q$ (Table 11) revealed the statistical significance of the developed QSAR models.

*Development of multi-target QSAR model*

According to the above ot-QSAR models one should use five different equations with different errors to predict the activity of a new compound against the five microbial species. The ot-QSAR models, which are almost in the whole literature, become unpractical or at less complicated to use when we have to predict to each compound results for more than one target. In these cases, we have to develop one ot-QSAR for each target. However, very recently the interest has been increased in development of multi-target QSAR (mt-QSAR) models. In opposition to ot-QSAR, the mt-QSAR model is a single equation that considers the nature of molecular descriptors which are common and essential for describing the antibacterial and antifungal activities (Prado-Prado *et al*., 2008; Gonzalez-Diaz *et al*., 2007, 2008; Cruz-Monteagudo *et al*., 2007; Gonzalez-Diaz and Prado-Prado, 2008).

In this study, we have attempted to develop three different types of mt-QSAR models viz. mt-QSAR model for describing antibacterial activity of synthesized compounds against *S. aureus*, *B. subtilis*, and *E. coli*, mt-QSAR model for describing antifungal activity of synthesized compounds against *C. albicans* and *A. niger* as well a common mt-QSAR model for describing the antimicrobial (overall antibacterial and antifungal) activity of synthesized isoniazid derivatives against all the above-mentioned microorganisms.

In order to develop mt-QSAR models, initially we have calculated the average antibacterial, antifungal, and antimicrobial activity values of isoniazid derivatives which are presented in Table 6. These average activity values were also correlated with the molecular descriptors of synthesized compounds (Table 9).

The mt-QSAR model for antibacterial activity displayed the importance of electronic energy (Ele.E) in describing the antibacterial activity of synthesized isoniazid derivatives, represented as the model expressed by Eq. 6.

*mt-QSAR model for antibacterial activity*

$$\mathrm{pMIC_b} = -0.0000192\ \mathrm{Ele.E} + 1.684 \quad (6)$$

$$n = 15, \quad r = 0.944, \quad q^2 = 0.852, \quad s = 0.063, \quad F = 106.40.$$

The mt-QSAR model for antifungal and antimicrobial activities revealed the importance of nuclear repulsion energy (Nu.E) in describing antifungal activity and the overall antimicrobial activity represented by Eqs. 7 and 8, respectively.

*mt-QSAR model for antifungal activity*

$$\mathrm{pMIC_f} = 0.0000191\mathrm{Nu.E} + 2.057 \quad (7)$$

$$n = 15, \quad r = 0.865, \quad q^2 = 0.636, \quad s = 0.093, \quad F = 38.88.$$

*mt-QSAR model for antimicrobial activity*

$$\mathrm{pMIC_{am}} = 0.0000204\mathrm{Nu.E} + 1.849 \quad (8)$$

$$n = 15, \quad r = 0.942, \quad q^2 = 0.835, \quad s = 0.061, \quad F = 03.09.$$

It was observed from mt-QSAR models (Eqs. 6–8) that the antibacterial, antifungal, and overall antimicrobial activities of synthesized isoniazid derivatives is governed by energy parameters, viz., nuclear repulsion energy (Nu.E) describing the antifungal and overall antimicrobial potential and electronic energy describing the antibacterial potential of the isoniazid derivatives. The developed mt-QSAR models were statistically valid as they had the high $r$ and $q^2$ values and low residual values (Table 12). As in the case of ot-QSAR models, the plot of predicted $\mathrm{pMIC_{am}}$ against observed $\mathrm{pMIC_{am}}$ (Fig. 4) also favors the developed model

**Table 12** Comparison of observed and predicted antibacterial, antifungal, and antimicrobial activities obtained by mt-QSAR model

| Compound | $pMIC_b$ (Eq. 6) | | | $pMIC_f$ (Eq. 7) | | | $pMIC_{am}$ (Eq. 8) | | |
|---|---|---|---|---|---|---|---|---|---|
| | Obs | Pre | Res | Obs | Pre | Res | Obs | Pre | Res |
| Training set | | | | | | | | | |
| **1** | 2.16 | 2.11 | 0.05 | 2.36 | 2.41 | −0.05 | 2.24 | 2.23 | 0.01 |
| **2** | 2.14 | 2.08 | 0.06 | 2.34 | 2.38 | −0.04 | 2.22 | 2.20 | 0.02 |
| **3** | 2.06 | 2.13 | −0.07 | 2.36 | 2.43 | −0.07 | 2.18 | 2.25 | −0.07 |
| **4** | 2.20 | 2.20 | 0.00 | 2.40 | 2.49 | −0.09 | 2.28 | 2.31 | −0.03 |
| **5** | 1.98 | 2.01 | −0.03 | 2.28 | 2.32 | −0.04 | 2.10 | 2.13 | −0.03 |
| **6** | 2.14 | 2.04 | 0.10 | 2.34 | 2.35 | −0.01 | 2.22 | 2.16 | 0.06 |
| **7** | 2.07 | 2.13 | −0.06 | 2.37 | 2.43 | −0.06 | 2.19 | 2.24 | −0.05 |
| **8** | 2.02 | 2.06 | −0.04 | 2.48 | 2.37 | 0.11 | 2.20 | 2.18 | 0.02 |
| **9** | 1.88 | 1.92 | −0.04 | 2.33 | 2.24 | 0.09 | 2.06 | 2.05 | 0.01 |
| **10** | 2.38 | 2.36 | 0.02 | 2.78 | 2.64 | 0.14 | 2.54 | 2.47 | 0.07 |
| **11** | 2.29 | 2.40 | −0.11 | 2.49 | 2.67 | −0.18 | 2.37 | 2.51 | −0.14 |
| **12** | 2.28 | 2.31 | −0.03 | 2.63 | 2.59 | 0.04 | 2.42 | 2.42 | 0.00 |
| **13** | 2.49 | 2.42 | 0.07 | 2.80 | 2.69 | 0.11 | 2.61 | 2.53 | 0.08 |
| **14** | 2.34 | 2.27 | 0.07 | 2.59 | 2.56 | 0.03 | 2.44 | 2.39 | 0.05 |
| INH | 1.84 | 1.84 | 0.00 | 2.19 | 2.17 | 0.02 | 1.98 | 1.98 | 0.00 |
| Test set | | | | | | | | | |
| **15** | 2.08 | 2.02 | 0.06 | 2.29 | 2.33 | −0.04 | 2.17 | 2.14 | 0.03 |
| **16** | 2.24 | 2.29 | −0.05 | 2.74 | 2.58 | 0.16 | 2.44 | 2.4 | 0.04 |
| **17** | 2.11 | 2.19 | −0.08 | 2.41 | 2.48 | −0.07 | 2.23 | 2.3 | −0.07 |
| **18** | 2.14 | 2.07 | 0.07 | 2.19 | 2.37 | −0.18 | 2.16 | 2.18 | −0.02 |
| **19** | 2.16 | 1.84 | 0.32 | 2.26 | 2.17 | 0.09 | 2.20 | 1.97 | 0.23 |

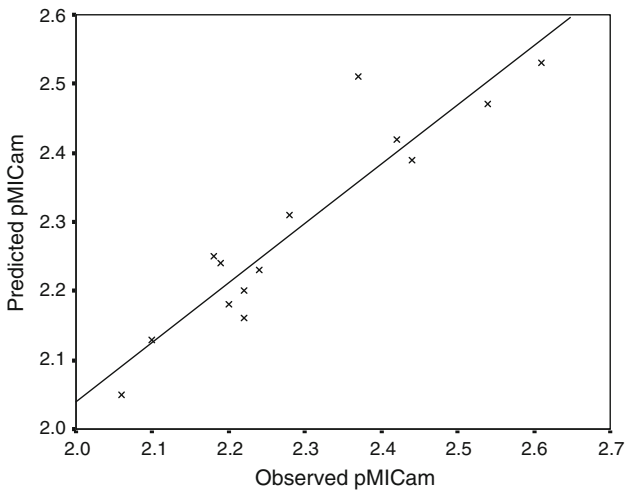


**Fig. 4** Plot of observed pMICam against the predicted pMICam for the linear regression model developed by Eq. 8

expressed by Eq. 8. Further, the plot of observed $pMIC_{am}$ versus residual $pMIC_{am}$ (Fig. 5) indicated that there was no systemic error in model development as the propagation of error was observed on both sides of zero, i.e., both positive and negative residual values were observed. The low value of

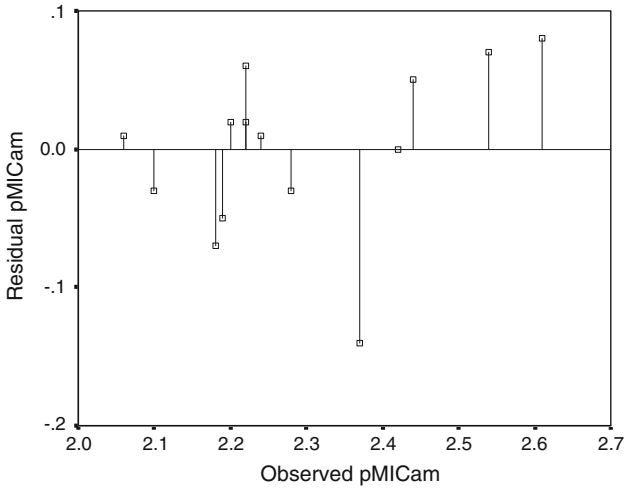


**Fig. 5** Plot of residual pMICam against the experimental pMICam for the linear regression model developed by Eq. 8

PE, LSE, LOF, standard deviation of prediction ($S_{press}$) and standard deviation error of predictions ($SD_{EP}$) and $SE_P$ and high value of $r^2$ and $Q$ (Table 11) revealed the statistical significance of the developed QSAR models.

## Validation of predictability of developed QSAR models using test set

In order to validate the predictability of the developed QSAR models, we have synthesized a test set of five compounds (**15–19**) and their antimicrobial activity values were determined experimentally as well as predicted using the developed QSAR models and the results are presented in Tables 10 and 12. The results of the predicted antimicrobial activity indicated that the developed models were efficiently predicting the antimicrobial activity of the synthesized compounds with similar structure (compounds **15** and **16**) as well as compound with slightly different structures (compounds **17–19**). The low residual values for these compounds indicated that the developed QSAR models were valid as they were predicting the antimicrobial activity quite effectively. The mt-QSAR models were more precise in prediction as their residual values were very low.

## Conclusion

A series of isoniazid derivatives (**1–19**) was synthesized and tested for their in vitro antimycobacterial activity against *M. tuberculosis* and the compounds with OH, $SCH_3$, and $OCH_3$ groups were found to be active ones and

compound **17** synthesized in the test set was twice active than ciprofloxacin and thrice active than ethambutol. The results of antiviral activity testing showed that none of the tested compounds was active against a broad variety of RNA and DNA viruses at subtoxic concentrations, except compound **8** that showed a selective anti-reovirus-1 activity. The synthesized compounds were also screened for their antimicrobial potential against *S. aureus, B. subtilis*, *E. coli*, *C. albicans*, and *A. niger* and the results of antimicrobial activity were similar to the antimycobacterial activity except that $N_1$-acyl substituted derivatives (**10**–**14**) were the most active antimicrobial agents. To understand the relationship between physicochemical parameters and antibacterial and antifungal activities of isoniazid derivatives, QSAR investigation was performed by development of one target and multi target models. The multi-target model was found to be effective in describing the antimicrobial activity of isoniazid derivatives in comparison to the one target models and indicated the importance of nuclear repulsion energy (Nu.E). The external validation of QSAR models was done by the prediction of antimicrobial activity of test set compounds.

**Acknowledgments** The author (VJ) is thankful to Department of Technical Education, Government of Haryana (India) for providing fellowship to carry out the research project. We would like to thank Mrs. Leentje Persoons, Mrs. Frieda De Meyer and Mrs. Leen Ingels, Rega Institute for Medical Research, Belgium for excellent technical assistance in the evaluation of antiviral activity.

## References

Bajaj S, Sambi SS, Madan AK (2005) Prediction of anti-inflammatory activity of *N*-arylanthranilic acids: computational approach using refined Zagreb Indices. Croat Chem Acta 78(2):165–174

Balaban AT (1982) Highly discriminating distance-based topological index. Chem Phys Lett 89:399–404

Bayrak H, Demirbas A, Demirbas N, Karaoglu SA (2009a) Synthesis of some new 1,2,4-triazoles starting from isonicotinic acid hydrazide and evaluation of their antimicrobial activities. Eur J Med Chem 44:4362–4366

Bayrak H, Demirbas A, Karaoglu SA, Demirbas N (2009b) Synthesis of some new 1,2,4-triazoles, their mannich and schiff bases and evaluation of their antimicrobial activities. Eur J Med Chem 44:1057–1066

Canoa P, Gonzalez-moa MJ, Teijeira M, Teran C, Uriarte E, Pannecouque C, De Clercq E (2006) Synthesis and anti-HIV activity of novel cyclopentenyl nucleoside analogues of 8-azapurine. Chem Pharm Bull 54(10):1418–1420

Cappucino JG, Sherman N (1999) Microbiology—a laboratory manual. Addison Wesley Longman Inc, Redwood City, p 263

Clementi E (1980) Computational aspects of large chemical systems. Springer, New York

Cruz-Monteagudo M, Gonzalez-Diaz H, Aguero-Chapin G, Santana L, Borges F, Dominguez ER, Podda G, Uriarte E (2007) Computational chemistry development of a unified free energy Markov model for the distribution of 1300 chemicals to 38 different environmental or biological systems. J Comput Chem 28(11):1909–1923

Dai J, Sun C, Han S, Wang L (1999) QSAR for polychlorinated compounds (PCOCs). I. Prediction of partition properties for PCOCs using quantum chemical parameters. Bull Environ Contam Toxicol 62:530–538

Desai B, Sureja D, Naliapara Y, Shah A, Saxena AK (2001) Synthesis and QSAR studies of 4-substituted phenyl-2,6-dimethyl-3,5-bis-*N*-(substituted phenyl)carbamoyl-1,4-dihydro- pyridines as potential antitubercular agents. Bioorg Med Chem 9:1993–1998

Emami S, Foroumadi A, Falahati M, Lotfali E, Rajabalian S, Ebrahimi FS, Shafiee A (2008) 2-Hydroxyphenacyl azoles and related azolium derivatives as antifungal agents. Bioorg Med Chem Lett 18:141–146

Golbraikh A, Tropsha A (2002) Beware of $q^2$!. J Mol Graphics Model 20:269–276

Gonzalez-Diaz H, Prado-Prado FJ (2008) Unified QSAR and network-based computational chemistry approach to antimicrobials, part 1: multispecies activity models for antifungals. J Comput Chem 29(4):656–667

Gonzalez-Diaz H, Vilar S, Santana L, Uriarte E (2007) Medicinal chemistry and bioinformatics—current trends in drugs discovery with networks topological indices. Curr Top Med Chem 7(10): 1015–1029

Gonzalez-Diaz H, Gonzalez-Diaz Y, Santana L, Ubeira FM, Uriarte E (2008) Networks and connectivity indices. Proteomics 8(4): 750–778

Guven OO, Erdogan T, Goker H, Yildiz S (2007) Synthesis and antimicrobial activity of some novel phenyl and benzimidazole substituted benzyl ethers. Bioorg Med Chem 17:2233–2236

Hansch C, Fujita T (1964) p-$\sigma$-$\pi$ analysis. A method for the correlation of biological activity and chemical structure. J Am Chem Soc 86:1616–1626

Hansch C, Leo A, Unger SH, Kim KH, Nikaitani D, Lien EJ (1973) Aromatic substituent constants for structure-activity correlations. J Med Chem 16:1207–1216

Hatya SA, Aki-sener E, Tekiner-Gulbas B, Yildiz I, Temiz-Arpaci O, Yalcin I, Altanlar N (2006) Synthesis, antimicrobial activity and QSARs of new benzoxazine-3-ones. Eur J Med Chem 41: 1398–1404

Hyperchem 6.0 (1993), Hypercube, Inc., Gainesville

Imramovsky A, Polanc S, Vinsova J, Kocevar M, Jampilek J, Reckova Z, Kaustova J (2007) A new modification of antitubercular active molecules. Bioorg Med Chem 15:2511–2559

Judge V, Narang R, Sharma D, Narasimhan B, Kumar P Hansch analysis for the prediction of antimycobacterial activity of ofloxacin derivatives. Med Chem Res. doi: 10.1007/s00044-010-9400-8 (in press)

Karelson M, Lobanov VS, Katritzky AR (1996) Quantum-chemical descriptors in QSAR/QSPR studies. Chem Rev 96(3):1027–1044

Kier LB, Hall LH (1976) Molecular connectivity in chemistry and drug research. Academic Press, New York

Kim YM, Farrah S, Baney RH (2007) Structure-antimicrobial activity relationship for silanols, a new class of disinfectants, compared with alcohols and phenols. Int J Antimicrob Agents 29:217–222

Koh Y, Nakata H, Maeda K, Ogata H, Bilcer G, Devasamudram T, Kincaid JF, Boross P, Wang Y, Tie Y, Volarath P, Gaddis L, Harrison RW, Weber IT, Ghosh AK, Mitsuya H (2003) Novel *bis*-tetrahydrofuranylurethane containing nonpeptidic protease inhibitor (PI) UIC-94017 (TMC114) with potent activity against multi-PI-resistant Human Immunodeficiency Virus in vitro. Antimicrob Agents Chemother 47(10):3123–3129

Kumar A, Sharma P, Gurram VK, Rane N (2006) Studies on synthesis and evaluation of quantitative structure–activity relationship of 10-methyl-6-oxo-5-arylazo-6,7-dihydro-5H-[1,3]azaphospholo

[1,5-d][1,4]benzodiazepin-2-phospha-3-ethoxycarbonyl-1-phosphorus dichlorides. Bioorg Med Chem Lett 16:2484–2491

Kumar A, Narasimhan B, Kumar D (2007) Synthesis, antimicrobial, and QSAR studies of substituted benzamides. Biorg Med Chem 15:4113–4124

Kumar P, Narasimhan B, Sharma D, Judge V, Narang R (2009) Hansch analysis of substituted benzoic acid benzylidene/furan-2-yl-methylene hydrazides as antimicrobial agents. Eur J Med Chem 44:1853–1863

Kumar D, Judge V, Narang R, Sangwan S, De Clercq E, Balzarini J, Narasimhan B (2010a) Benzylidene/2-chlorobenzylidene hydrazides: synthesis, antimicrobial activity, QSAR studies and antiviral evaluation. Eur J Med Chem 45:2806–2816

Kumar P, Narasimhan B, Yogeeswari P, Sriram D (2010b) Synthesis and antitubercular activities of substituted benzoic acid *N*′-(substituted benzylidene/furan-2-ylmethylene)-*N*-(pyridine-3-carbonyl)-hydrazides. Eur J Med Chem 45:6085–6089

Lather V, Madan AK (2005) Topological models for the prediction of anti-HIV activity of dihydro (alkylthio) (napthylmethyl) oxo-pyrimidines. Bioorg Med Chem 13:1599–1604

Mandloi D, Joshi S, Khadikar PV, Khosla N (2005) QSAR study on the antibacterial activity of some sulfa drugs: building blockers of Mannich bases. Bioorg Med Chem Lett 15:405–411

Manna K, Agrawal YK (2010) Design, synthesis, and antitubercular evaluation of novel series of 3-benzofuran-5-aryl-1-pyrazolyl-pyridylmethanone and 3-benzofuran-5-aryl-1-pyrazolylcarbonyl-4-oxo-naphthyridin analogs. Eur J Med Chem 45:3831–3839

Narasimhan B, Judge V, Narang R, Ohlan S, Ohlan R (2007) Quantitative structure–activity relationship studies for prediction of antimicrobial activity of synthesized 2,4-hexadienoic acid derivatives. Bioorg Med Chem Lett 17:5836–5845

National Committee for Clinical Laboratory Standards (1995) Antimycobacterial susceptibility testing for *Mycobacterium tuberculosis*. Proposed standard M24-T. National Committee for Clinical Laboratory Standards, Villanova

Nayyar A, Monga V, Malde A, Coutinho E, Jain R (2007) Synthesis and anti-tuberculosis activity, and 3D-QSAR study of 4-(adamantan-1-yl)-2-substituted quinolines. Bioorg Med Chem 15:626–640

Pauwels R, Balzarini J, Baba M, Snoeck R, Schols D, Herdewijn P, Desmyter J, De Clercq E (1988) Rapid and automated tetrazolium based colorimetric assay for detection of anti-HIV compounds. J Virol Methods 20:309–322

Pharmacopoeia of India (2007) Controller of Publications, vol I. Ministry of Health Department, Govt. of India, New Delhi, p 37

Pinheiro AAC, Borges RS, Santos SL, Alves CN (2004) A QSAR study of 8.O.4′-neolignans with antifungal activity. J Struct Mol (Theochem) 672:215–219

Prado-Prado FJ, Gonzalez-Diaz H, Vega OMDL, Ubeira FM, Chou KC (2008) First multi-tasking QSAR model for Input-Coded prediction, structural back-projection, and complex networks clustering of antiprotozoal compounds. Bioorg Med Chem 16(11):5871–5880

Randic M (1975) Characterization of molecular branching. J Am Chem Soc 97:6609–6615

Randic M (1993) Comparative regression analysis. Regressions based on a single descriptor. Croat Chem Acta 66:289–312

Rodriguez-Arguelles MC, Lopez-Silva EC, Sanmartin J, Pelagatti P, Zani F (2007) Copper complexes of imidazole-2-, pyrrole-2- and indol-3-carbaldehyde thiosemicarbazones: inhibitory activity against fungi and bacteria. J Inorg Biochem 101:138–147

Sabet R, Mohammadpour M, Sadeghi A, Fassihi A (2010) QSAR study of isatin analogues as in vitro anti-cancer agents. Eur J Med Chem 45:1113–1118

Sbardella G, Mai A, Artico M, Setzu MG, Poni G, Colla PL (2004) New 6-nitroquinolones: synthesis and antimicrobial activities. IL Farmaco 59:463–471

Schaper KJ (1999) Free-Wilson-type analysis of non-additive substituent effects on THPB dopamine receptor affinity using artificial neural networks. Free-Wilson-type analysis of non-additive substituent effects on THPB dopamine receptor affinity using artificial neural networks. Quant Struct Act Relat 18: 354–360

Scior T, Garces-Eisele SJ (2006) Isoniazid is not a lead compound for its pyridyl ring derivatives, isonicotinoyl amides, hydrazides, and hydrazones: a critical review. Curr Med Chem 13(18): 2205–2219

Sharma P, Kumar A, Sharma M (2006) Synthesis and QSAR studies on 5-[2-(2-methylprop-1-enyl)-1Hbenzimidazol-1yl]-4,6-diphenyl-pyrimidin-2-(5H)- thione derivatives as antibacterial. Eur J Med Chem 41:833–840

Sivaprakasam P, Xiea A, Doerksen RJ (2006) Probing the physicochemical and structural requirements for glycogen synthase kinase-3a inhibition: 2D-QSAR for 3-anilino-4-phenylmaleimides. Bioorg Med Chem 14:8210–8218

Sortino M, Delgado P, Jaurez S, Quiroga J, Abonia R, Insuasey B, Rodero MN, Garibotto FM, Enriz RD, Zacchino SA (2007) Synnthesis and antifungal activity of (Z)-5-arylidenerhodanines. Bioorg Med Chem 15:484–494

SPSS for Windows (1999) version 10.05, SPSS Inc., Bangalore

Sriram D, Yogeeswari P, Madhu K (2006) Synthesis and in vitro antitubercular activity of some 1-[(4-sub)phenyl]-3-(4-{1-[(pyridine-4-carbonyl)hydrazono]ethyl} phenyl thiourea. Bioorg Med Chem Lett 16:876–878

Sriram D, Yogeeswari P, Dhakla P, Senthilkumar P, Banerjee D (2007) N-Hydroxythiosemicarbazones: synthesis and antitubercular activity. Bioorg Med Chem Lett 17:1888–1891

Sriram D, Yogeeswari P, Priya DY (2009) Antimycobacterial activity of novel N-(substituted)-2-isonicotinoylhydrazinocarbothioamide endowed with high activity towards isoniazid resistant tuberculosis. Biomed Pharmcother 63:36–39

Tripathi RP, Saxena N, Tiwari VK, Verma SS, Chaturvedi V, Manju YK, Srivastva AK, Gaikwad A, Sinha S (2006) Synthesis and antitubercular activity of substituted phenylmethyl- and pyridylmethyl amines. Bioorg Med Chem 4:8186–8196

TSAR 3D Version 3.3 (2000), Oxford Molecular Limited

Wiener H (1947) Structural determination of paraffin boiling points. J Am Chem Soc 69:17–20